152604

SOLAR RADIO ASTRONOMY

2-8 GHz SOLAR DYNAMIC SPECTRA AND POLARIZATION MEASUREMENT FEASIBILITY STUDY

FRED T. HADDOCK

THE UNIVERSITY OF MICHIGAN
RADIO ASTRONOMY OBSERVATORY
ANN ARBOR, MICHIGAN 48104

FEBRUARY 1971
FINAL REPORT FOR PERIOD
NOVEMBER 1970 - FEBRUARY 1971

PREPARED FOR

GODDARD SPACE FLIGHT CENTER
GREENBELT, MARYLAND 20771

TECHNICAL REPORT STANDARD TITLE PAGE

1. Report No.	2. Government Accession No.	3. Recipient's Catalog No.

4. Title and Subtitle	5. Report Date
"Solar Radio Astronomy", 2-8 GHz Solar Dynamic Spectra and Polarization Measurement Feasibility Study	6. Performing Organization Code

7. Author(s)	8. Performing Organization Report No.
Fred T. Haddock	UM/RAO No. 71-3

9. Performing Organization Name and Address	10. Work Unit No.
Radio Astronomy Observatory The University of Michigan Physics & Astronomy Building Ann Arbor, Mich. 48104	11. Contract or Grant No. NAS5-11344

12. Sponsoring Agency Name and Address	13. Type of Report and Period Covered
NASA/Goddard Space Flight Center Greenabelt, Maryland 20771 Technical Monitor: Dr. R. G. Stone Code 615	Final Nov. 1970-Feb. 1971
	14. Sponsoring Agency Code

15. Supplementary Notes

16. Abstract

This report contains the preliminary system design of a Solar Microwave Spectrograph (SMS) which resulted from a four month independent study to determine the feasibility of measuring solar polarization and dynamic spectra over the range of two to eight GHz, using broadband radio frequency instrumentation and rapid recording equipment in conjunction with the radio telescopes of the University of Michigan Radio Astronomy Observatory. This report also contains a discussion of the scientific value of the proposed SMS instrument, a brief discussion of data reduction and analysis, and a clear and concise presentation of the engineering plan to implement the SMS system.

17. Key Words (Selected by Author(s))	18. Distribution Statement
SOLAR MICROWAVE SPECTROGRAPH	

19. Security Classif. (of this report)	20. Security Classif. (of this page)	21. No. of Pages	22. Price*
Unclassified	Unclassified	172	

PREFACE

(A) Objective:

The University of Michigan Radio Astronomy Observatory conducted a four month independent study of the feasibility of measuring solar polarization and dynamic spectra over a range of two to eight GHz, using broadband r.f. instrumentation and rapid recording equipment associated with the 28-foot and 85-foot radio telescope. This study was performed in accordance with the contractor's proposal ORA 70-1461-KB1, dated May 1970, entitled "Proposal to National Aeronautics and Space Administration Solar Radio Astronomy" and NASA/GSFC Contract No. NAS 5-11344 starting 1 November 1970. This final report on the study is the preliminary system design of a Solar Microwave Spectrograph.

(B) Scope of Work:

(1) The study included a determination of the uniqueness and scientific value of the proposed measurement system, (2) the system design effort necessary to obtain a clear and concise statement of the engineering definition of the measurement system, (3) the resource requirements necessary to implement the measurement system, (4) trade-offs which would be possible as a function of available

resources, (5) an estimate of the operational costs to support the measurement system and to reduce the data, and (6) a plan to utilize available resources to complete the construction of the measurement system.

(C) Conclusions:

A solar polarization and dynamic spectra measurement system has been defined which will satisfy the scientific goals, is well within the state-of-the-art, has inherent flexibility (as exhibited by the many trade-offs), and can be constructed in a timely manner (approximately 18 months).

(D) Summary of Recommendations:

This solar measurement system should be constructed and operated since there is a definite need for highly accurate temporal measurements of solar polarization and dynamic spectra in this frequency range.

CONTENTS

CONTENTS (Continued)

CONTENTS (Continued)

LIST OF FIGURES

LIST OF TABLES

1. INTRODUCTION

This is the final report of a four month independent study of the feasibility of measuring solar polarization and dynamic spectra over the range of two to eight GHz. The system that is proposed would use broad-band radio-frequency instrumentation and rapid recording equipment in conjunction with the radio telescopes of the University of Michigan Radio Astronomy Observatory (UM/RAO) to obtain these measurements.

This report contains a discussion of the scientific value of the proposed Solar Microwave Spectrometer (SMS) instrument, a brief discussion of data reduction and analysis, and a clear and concise presentation of the engineering plan to implement the SMS system.

2. SCIENTIFIC GOALS

INTRODUCTION TO SCIENTIFIC DISCUSSION

This study is to determine the feasibility of an ultra rapid, high data rate microwave spectrometer-polarimeter for precision measurement of solar bursts. There are two key objectives for this instrument. First, to obtain solar microwave burst data for detailed comparisons with associated solar x-ray bursts data, which should eventually become available with comparable completeness and precision, from the OSO satellite series. Second, to obtain rapidly (120 K bit/sec) data of such completeness in temporal, spectral, and intensity resolution, in accuracy of intensity for two states of polarization over the full range of burst intensities, and with high detection sensitivity so that a significant advance in the quantitative understanding of solar microwave radiation becomes highly probable, even without data from other frequency regions.

2.1 INSTRUMENT DESIGN AND THE SCIENTIFIC OBJECTIVES

The essential features of this system are: a large collecting area antenna (28-ft or 85-ft); twenty discrete and contiguous frequency channels from 2 GHz (λ15 cm) to 8 GHz (λ3.75 cm) each with a 7% bandpass; a switch time of 0.2 millisecond (msec) between right-hand and left-hand circular polarization; recording of the full range of burst intensities with a uniform 1% accuracy on magnetic tape of

all 20 channels every 2 msec; semi-automatic control of the system, including the decision to store at maximum rate or at a reduced rate using running averages; tape units that are replicated to avoid loss of recorded data; precision calibration of receivers over the full dynamic range; and absolute calibration of the complete system using known discrete radio sources, Cas A, Cyg-A, Crab Nebula, Orion Nebula, etc. The mode of operation can be chosen from a variety of arrangements. The time resolution could be increased to 0.2 ms by recording only two channels or the detection sensitivity could be increased after the event by reducing spectral or temporal resolution or both, etc.

The instrument proposed however, does <u>not</u> have sufficient angular resolution to be of direct value in the study of radio bursts, although it indirectly contributes to system sensitivity. The half-intensity beamwidth, W, of the 28-ft paraboloid is 144 f^{-1}, and for the 85-ft, W = 48 f^{-1}, where W is in units of minutes of arc and f is the channel frequency in units of 10^9 Hz or GHz. The beamwidths can be expressed in solar diameters as w = 4.5 f^{-1} and 1.5 f^{-1}, respectively. Thus at frequencies above 4.5 GHz and 1.5 GHz the beam becomes smaller than the sun, for the 28-ft and 85-ft antennas, respectively. However even at 8 GHz with the 85-ft antenna the beam is 6' arc, which is still large compared to an active region. In fact, at this extreme the beam sharpness may be a nuisance because

it requires better beam location and tracking accuracy to keep on a selected active region. Furthermore the greater collecting area, compared to the 28-ft antenna, is not always an important advantage when the system noise level is determined primarily by the selected active region enhanced radiation since the region is smaller than the beam. This situation will be discussed later.

2.1.1 Spatial Resolution. Angular resolution measurements of microwave bursts would be very important if capable of resolving the size and structure of the burst, expecially if made rapidly and without spatial ambiquity. To accomplish this requires a multi-antenna system of considerable cost and complexity. Since the Japanese have already obtained a 1.6' x 2.4' arc elliptical beam at 9.4 GHz (λ3.18 cm) using 48 paraboloids and a 0.4' arc fan beam using 34 paraboloids at 3.75 GHz (λ8 cm), an additional instrument in this frequency range should have significantly higher resolution, about 0.4' x 0.6' elliptical beam or a 0.1' arc fan beam in order to justify the considerable cost, time, and effort. Therefore we have abandoned angular resolution in this proposal in favor of temporal, spectral, polarization, and intensity resolution, high sensitivity, frequency coverage and reduced costs.

The loss of angular resolution on bursts does not preclude all spatial resolution. Spatial resolution on rapid dynamic events can be obtained by fine angular discrimination or by fine time discrimination. Although not always unambiguous, it is possible to set upper limits on the linear source size of impulsive bursts by the light travel time smoothing effect on the received pulse shape. This analysis has received considerable discussion in the literature on quasi-stellar sources, especially the radio variability which was discovered by Dent in 1965 in our group.

A radio burst of duration Δt could not arise from a region larger, in the line of sight, than $u\Delta t$, where u = group velocity in the medium. Since $u \leq c$ the size is less than the corresponding light distance $c\Delta t$. (c = 300 km/msec) If the burst duration were 2.4 msec the light distance scale of source region would be less than 725 km. At the sun 725 km normal to the line of sight subtends 1 sec of arc. Table 1 gives the equivalent scales of size at the sun for comparison of the time resolution, Δt, with the angular resolution , $\Delta\theta$, where L is the corresponding linear scale. In one case L is normal to and the other case parallel to the

line of sight. The proposed instrument can just resolve at 20 frequencies and two polarizations source sizes of 1" arc or 725 km, corresponding to 2.4 msec, if the source were sufficiently bright.

If x-ray burst events have temporal features and the instrumental resolution were comparable to the microwave values then measurements of x-ray and radio source coincidence to within 1000 km would be feasible.

Table 1 Equivalent Scales of Size at the Sun

L (km)	Δt (msec)	$\Delta\theta$ (min of arc)
696,000	2320	16
43,500	145	1
4,350	14.5	1/10
725	2.5	1/60

If a single source of acceleration of fast particles at the top of an arch of magnetic field lines ejected the particles outward in opposite directions along the field lines until they struck denser chromospheric gas or magnetic mirror points where

they then emitted radio bursts, the delay time in the arrival of the bursts at the earth would be equal to the light travel time difference in their paths to the earth. The value would depend on the heliographic location of the arch and its size. For an east-west arch on the limb of the sun the time delay between these oppositely polarized bursts could be 300 msec.

2.1.2 Minimum Detectable Burst Flux Density. It is now necessary to discuss the minimum source size that could be detected with this instrument if we are limited to an integration period of 2.4 msec. First we need the minimum detectable flux level. The signal-to-noise ratio is $S/N = \frac{sF_B}{mF_s}$ when the beam, W, is larger than the microwave solar diameter 35' arc (at microwaves the radio diameter is a few min of arc larger than the visible disk). F_B is the burst flux density in solar flux density units (f.u.) equal to 10^{-22} W/m^2 Hz, $F_s = 25\ f$ is the quiet sun flux density in solar flux units, f is the channel frequency in GHz, $2 \leq f \leq 8$, m is the enhancement factor of the actual sun over the sunspot minimum value; m can approach 3 or 4 during maximum. $s = (\Delta\nu \cdot \tau)^{1/2} = 408\ f^{1/2}$ is the statistical smoothing factor due to integration

time τ = 2.4 msec and the channel bandwidth $\Delta\nu = 0.0693 \times 10^9$ f, since the bandwidth is determined by exactly 10 channels per octave equally spaced on a log scale. Thus the ratio of adjacent channel frequencies is R, where $R^{10} = 2$, or R = 1.071773. The bandwidth to arithmetic mean channel frequency is

$$2\left(\frac{\nu_2 - \nu_1}{\nu_2 + \nu_1}\right) = 2\left(\frac{R - 1}{R + 1}\right) = 0.069287 .$$

Therefore, $S/N = \frac{408\ f^{1/2}\ F_B}{25\ m\ f} = \frac{16.32\ F_B}{m\ f^{1/2}}$

Assuming a minimum S/N = 3 and m = 2, we have for the minimum detectable burst, $F_B(\text{min}) = 0.37\ f^{1/2}$ f.u. At 8 GHz we have $F_B(\text{min})$ = 1.05 f.u. and at 2 GHz, 0.52 f.u., using small antennas.

When the beam is smaller than the sun the S/N is improved by a factor $\left(\frac{35'}{W'}\right)^2$, if the sun has no strong active regions in the beam. The 28-ft antenna at 8 GHz has W = 18', thus giving a factor of 3.8 improvement in S/N. Then $F_B(\text{min})$ = 0.3 f.u., using the 28-ft antenna. $F_B(\text{min})$ = 0.03, using the 85-ft antenna. At the low end of the frequency range, 2 GHz, W > 35' and $F_B(\text{min})$ = 0.52 f.u., using the 28-ft antenna and 0.26, using the 85-ft, since W = 24'. Above 4.5 GHz both the 28- and 85-ft antenna

have beams smaller than the sun but larger than the selected, or targeted, active region. The flux density of active regions alone over the 2-8 GHz range varies from 22 to 26 f.u. with the peak value near 3 GHz.

It can be shown that for $4.5 \leq f \leq 8$ the S/N ratio for the 85-ft ranges from 4.2 to 5.7 times higher than for the 28-ft antenna. If the enhanced flux density from the unresolved active regions were neglected, then the 85-ft antenna S/N ratio would be equal to $(85/28)^2$, or 9.2, times that of the 28-ft antenna.

For $f < 4.5$, the ratio favoring the 85-ft will decrease as f decreases because the 28-ft beam is no longer completely on the solar disk.

For burst flux density values several times that of the solar disk and active region level, the advantage of the 85-ft antenna over the 28-ft disappears.

In conclusion we find that we can detect bursts down to 0.6 f.u., using either antenna.

2.1.3 Minimum Detectable Burst Size. How is source size and brightness related to the received flux density? Using equivalent black-body brightness temperature T_B and a circular source of diameter θ' arc we find that $F_B = 2 \times 10^{-7} f^2 T_B \theta^2$, f.u.

As f varies from 2 to 8 GHz, F_B varies from $8.15 \times 10^2 \theta^2$ to $1.3 \times 10^4 \theta^2$, f.u. when $T_B = 10^9$ K. For F = 1 f.u., θ = 2.1" to 0.53", respectively. This value of T_B is observed in microwave bursts of great intensity (10,000 f.u.) and with measured sizes of 2.5' arc, at 2.8 GHz. A 1 f.u. burst with $T_B = 10^9$ K would have a size of 1.5" arc at 2.8 GHz. This 1 f.u. burst could rise to maximum intensity in less than 4 msec. A 10^9 K source giving 1 f.u. at 8 GHz would have a size ~ 0.5" arc and could have a rise time of 1.2 msec. Thus we can detect burst sizes down to about 1" arc. Here is the reason for specifying a system time resolution of the order of 1-2 msec.

2.1.4 Precision Measurement of Spectral Index. How precisely can the burst spectrum be measured with this instrument? Assume that the spectrum is a linear on log F vs log f plot. That is, a power-law spectrum, $F = A f^{\alpha}$. The spectral index,

$$\alpha = \frac{\log F_{i+n} - \log F_i}{n \log R}$$

where F_i = flux density in the i - th channel and $R = f_{i+1}/f_i$, with $\log R = 0.1 \log 2 = 0.0301$.

Let F_i be measured with a relative accuracy of $a = \frac{\Delta F}{F}$, then the uncertainty in $\log F_i$ is $\log (1 \pm a) \cong \pm Ma$ (if $a < .05$), where $M = \log e = 0.43429$. Thus the uncertainty in α is

$$\Delta\alpha = \frac{\sqrt{2}\, M\, a}{n \log R} = \frac{20.4a}{n}$$

for $a < .05$. This simple expression is based on using flux values observed in only <u>two</u> channels spaced n channels apart, with a frequency separation ratio of R^n. Since the specified instrument intensity resolution is 1%, we have $\Delta\alpha = (\frac{20}{n})\%$. If the flux values at all n + 1 channels were used then $\Delta\alpha$ would be reduced. If n = 10 (an octave separation) and a = 1%, then $\Delta\alpha$ = 2%. This is a very high accuracy for spectral index measurements.

The values of α expected in microwave bursts varies from 1 to 7 on the low-frequency side of microwave spectra and from 0 to 22, with a peak at 7, on the high-frequency side, according to Castelli and Guidice (Fall URSI meeting, 1970, O.S.U.) If the emission process were synchrotron radiation

from a power-law electron energy distribution given by $N(E) = KE^{-\gamma}$, α would be $(\gamma - 1)/2$. Thus $\gamma = 2\alpha + 1$. For $\alpha = 7$, $\gamma = 15$. The uncertainty in γ would be $\Delta\gamma = 2\Delta\alpha = (40/n)\%$, this equals only 4% for $\gamma = 10$ (use of two channels an octave apart). This is also high accuracy for measuring γ. If 20 channel data were used then it would be possible to measure α in four steps over the 2 to 8 GHz band with an accuracy on α of 4%.

If the low-frequency side of the spectrum has an exponential cut-off due to free-free absorption, for example, then over an octave band it would be possible to discriminate between it and a power-law spectrum if its approximate power-law slope were greater than only 0.2. Therefore, in almost all cases it would be easy to identify power-law or exponential spectra with high reliability. Further, this could be done every few milliseconds, so that a rapidly changing spectrum could be measured and classified.

2.1.5 Possible Determination of Electron Acceleration Parameters. To record fully the explosive phase of the non-thermal components of a flare we require a time resolution of 1-2 msec to avoid averaging out with time the rising or variable flux curve at

detectable increments in intensity and to determine rapid changes in the spectrum. Since this instrument can record simultaneously at 20 frequencies at this time resolution in different polarization senses we should be able to measure and identify changes in the emitted radio spectrum during the first few tens of milliseconds above the minimum detection level and continuously thereafter. X-ray bursts show a harder spectrum on burst peaks than in the valleys, similar effects may appear in fast dynamic spectra of impulsive microwave bursts. It is this capability of measuring the rapidly changing intensity and polarization spectra well before the burst maximum occurs that offers a possible method of characterizing the non-thermal particle acceleration parameters and identifying the acceleration mechanism. Such an achievement would be a major contribution to solar physics. "Solar particle acceleration remains perhaps the most important unsolved problem in the study of solar cosmic rays." [Fichtel and McDonald (1967)].

2.1.6 Periodic Bursts. Another principal scientific objective is the study of the periodic repetitive burst trains which Parks and Winkler discovered in the x-ray solar bursts. They also found that the

associated microwave bursts exhibited the same period and synchronized in time. This is a remarkable finding and may provide the needed clue to understanding the radio and x-ray emission mechanism. Cribbins and Matthews found 14 periodic radio pulse trains at 2.8 GHz with periods from 6 to 600 sec. They discovered that the log P vs log F(max) plot gave a strong correlation between the period, P and the burst maximum flux density, F_{max}. We find a good fit to the data with

$$P^3 = \left(\frac{F(max)}{10}\right)^4 .$$

If we extrapolate their data down to the instrumental limit of measuring F(max) ≈ 1 f.u., then the corresponding pulse periods are near $P = 10^{-4/3} = 46$ msec. Since this is within the range of capability of our instrument we should be able to extend the observations from 6 sec to 46 ms, over two decades.

If we assume that the flares and microflares giving rise to periodic bursts are due to sudden expansions and collapse of the magnetoionic plasma with the restoring force (following Cowling) equal to $\frac{\pi y B^2}{\lambda^2}$, where y is the amplitude or radius of the expanded region, B the local uniform field, λ the characteristic scale or wavelength of the corresponding

Alfvén wave, then the period $P \sim \lambda/V_a$, where V_a is the Alfvén velocity in the flare region ($\sim 10^5$ km/s). If $\lambda \sim 10^5$ km ($\theta \sim 2.3'$ at the sun), then $P \sim 1$ sec. Thus, if P = 46 ms, the scale $\lambda \sim 4600$ km ($\theta \sim 6.3''$ arc).

This rough estimate indicates that rapid pulse trains may exist but have not been detected because of lack of sensitivity and time resolution. This instrument is ideally designed to detect and measure such expected events.

2.1.7 Data Display Plan. The data display is planned to be highly flexible since it is all under computer control. We will use displays already developed by our group under our OGO-I-V series of experiments. These include digital simulation of a sweep-frequency dynamic spectra display of frequency-time plot with the film density proportional to the burst intensity. The R.H. and L.H. circular polarization displays can be alternated or the (RH-LH)/(RH+LH) intensity can be displayed, etc. This gives a good overall view of the broadband burst event. The time and the intensity scales can be contracted and expanded for various uses, the intensity scale can be log or linear, it can be clipped above or below fixed levels, etc.

A display of precision time profiles of the average intensity over one or more channels of one or both polarizations will be plotted to make inspection of fine time variations easy. These time profiles will be cross correlated with periodic filters to search for periodicities in the data near the detection limit.

A display of intensity and polarization spectra will be made at selected times, chosen from the general dynamic spectra display or from the time profile display.

This should give an idea of the data display possibilities of this system.

2.1.8 Instrument Expansion Capability. The instrument has been designed for versatility and is easily expanded.

It appears that the majority of bursts which occur in the 2-8 GHz region are C type[1] bursts which tend to have maxima in the S and C band region. C type bursts which have maxima in the X or K_u band region could cause some confusion as to whether the burst was a C type with maximum above 8 GHz or an A type when spectral data is only available in the 2-8 GHz range. Therefore a logical

extension of the Solar Microwave Spectrograph (SMS) is a receiving system to cover the 8-16 GHz octave. Unfortunately, at frequencies above 8 GHz, microwave devices no longer cover octave bandwidths but rather cover waveguide bands (e.g. 8.2-12.4 GHz, 12-18 GHz, ...). Although it leaves a "hole" in the frequency coverage from 8-12 GHz[2], it appears that a receiver operating in the 12-18 GHz frequency band would provide additional valuable spectral information. A full description of the engineering aspects of the recommended expansion is in Section 3.6.1 .

Greater time and frequency resolution may be necessary but we cannot now predict and do not expect that either will be required. The presently proposed system should provide the information as to whether they are necessary or not.

---

[1]Castelli and Guidice use this microwave burst spectra classification. C_x means an inverted U-shape spectrum with maximum intensity in the X-band frequency, C type spectra constitute 80% of all microwave bursts. Spectra with $\alpha < 1$ (flux proportional to ν^{α}) are called type G, with $\alpha > 1$ are type A, and complex spectra are assigned to miscellaneous type. About 20% of bursts are Type G and very few (<<1%) are type A.

[2]See note at end of Section 3.6.2.

2.2 EXPERIMENTAL BACKGROUND

2.2.1 Time and Spectral Behavior. Microwave impulsive radio bursts are flare associated sudden increases in the solar noise level which peak in a time of the order of one minute after start and then decay so that the entire event is over in less than about five minutes. They may be predecessors of subsequent bursts of different types.

Microwave impulsive bursts have been observed at fixed frequencies over the frequency range of 1 to 15 GHz. Starting time, time of occurrence of peak flux and total burst duration on all the wavelengths are found to be quite close (within seconds of each other), and there is some similarity even in the fine structure. Typical spectra at any time during the burst are simple curves concave downward and usually with the peak flux occurring at a particular frequency (in the range of 2 to 16 GHz) with most peaks at about 5 GHz, independent of time. This is not always true and some bursts present a definite drift of the frequency of maximum flux toward lower values as the burst proceeds. The rate of shift of this peak is not always uniform. An example of more complex spectral shape is in Takakura and Kai (1966). These curves are slightly concave upward at the lower frequency end of the spectra well away from the frequency of peak flux until about 2 minutes after the burst maximum.

The shortest receiver time constants used have been of the order of 0.5 sec and the highest resolution has been of the order of 1.1 min. of arc.

2.2.2 Simultaneous Hard X-ray Bursts. A large number of these bursts have been associated with simultaneous bursts of solar X-ray emission measured by equipment which integrates the X-ray flux above either 10, 20 or 50 Kev, or in the range, for example, of 10-50 Kev. The starting times, times of maximum flux decay rates and integrated fluxes have correlated very well between the X-ray bursts and the microwave radio emission. In addition, a large number of these X-ray bursts show fine structure throughout the burst very similar to the fine structure in the corresponding radio bursts. A particularly striking example is an event of August 8, 1968 which showed 16-sec periodic pulsations in the >20 Kev X-ray burst closely correlated with a similar 16-second modulation in a 15.4 GHz record of the corresponding radio burst (Parks and Winckler 1969). The 16-second periodicity on this particular burst has also been observed at 2.7 GHz and 3.0 GHz [Janssens and White III (1969)].

A very striking study of periodic structure in bursts at 2.8 GHz is given by Cribbens and Matthews (1969). These authors found excellent linear correlation between log of the period length and log of the peak intensity of the burst and even better linear correlation between log of the period length and log of the total burst energy. From their data one finds that $P = (S/10)^{1.3}$ where P is the period and S is the peak flux in flux units (1 f.u. = $10^{-22} Wm^{-2} Hz^{-1}$). Unfortunately there appears to be no similar published data at other frequencies, microwave or X-ray.

The data on the nine flare events where simultaneous hard X-ray and centimeter wave bursts records were available, prior to 1962, are summarized by Kundu (1964, 1965). Since that time many more such simultaneous X-ray and radio events have been observed, thanks mainly to the X-ray experiments on the OGO-I and OGO-III satellites during Sept. 1964 to July 1966. These are reported by Arnoldy, Kane and Winckler (1967) who conducted the X-ray experiments and used radio data

from many sources. Further high correlations between X-ray burst fluxes above 2.7 Kev and cm radio bursts in June and July 1967 are reported by Harries (1970).

Further detailed evidence of this X-ray radio correlation for an event of June 9, 1968 is obtained by comparing the X-ray data presented by Kahler et. al. (1970) with the radio data given by Badillo and Castelli (1969).

2.2.3 High Spatial Resolution Observations. High resolution radio observations at 1, 2, 3.75, 0.4 GHz of impulsive bursts have been made by interferometers at Toyokawa Observatory with extensive results published by Tanaka and Enomé (1970), and in various earlier papers and reports. These observations are made using interferometers with fan beams whose half-power beam width = 1.1 min of arc in the east-west direction. Both total flux and the right- and left-hand circular polarization components were recorded. The 9.4 and 3.75 GHz interferometers have a quick scanning feature so that they scan the sun every 10 sec.

These observations show that the sources are localized in the east-west direction and moreover in a few cases are double sources. There appears to be no published statistics on the ratio of double to total number of sources observed. The double sources are two closely spaced regions separated by 0.5' and 4' of arc. There is a time delay of a few seconds in

the commencement of the bursts from each of the two regions and the polarization behavior of the radiation from each region is different.

2.2.4 Polarization Observations. Simultaneous observations at several frequencies at the Toyokawa Observatory and elsewhere (with no spatial resolution) have shown that many of the sources are polarized, the polarization is circular and that there is a shift in polarization sense from right to left,or conversely,with increasing frequency. For the double sources the polarization crossover occurs at different frequencies for each source region, but frequently in the frequency range of 2 to 10 GHz.

The high resolution feature of the Japanese observations has permitted statistical studies to be made of the effect on peak intensity and degree of polarization of center to limb variation of the source location [Takakura and Scalise Jr., (1970)]. The effects are small.

In addition to the high spatial resolution data there are extensive 7-GHz observations of total flux and polarization sense and degree made at Mackenzie University, São Paulo, Brazil [Kaufmann (1969), Kaufmann, Matsuura and Marques Dos Santos (1970)]. These are made with a 1.5° beam so there is no spatial resolution. In the latter paper the time history of 13 simple bursts

with well defined polarization were studied. The main features were that a peak in the degree of polarization occurred rapidly prior to the time of maximum flux. After an initial decay from this peak, the degree of polarization would usually enter into a gradual increase as the total flux decayed.

An appreciable fraction of the burst events are apparently not polarized. Kaufmann (1969) reported that about 18% of the impulsive bursts observed by the Brazilian 7 GHz radiometer had a polarization degree less than 0.3%. He examined a selected group of such events for which there was data available at other frequencies and for which the 7 GHz maximum flux exceeded 10 f.u. He found the spectra at the time of peak flux did not adequately fit into the types shown by Takakura and Kai (1966) nor into certain other classifications. There seems to be no other study of the spectra of these unpolarized bursts.

2.2.5 Polarization Fluctuation Bursts. A type of burst amenable to study by our proposed system has been observed on the 7-GHz radiometer in Brazil (Kaufmann, et. al., 1968). These bursts involve a constant flux level with only the degree of circular polarization changing. There are short impulsive bursts of this type lasting only 3 or 4 minutes and also longer bursts of the order of 30 minutes.

The data presented is sketchy and varied but indicates that this might well be a fruitful type of burst for spectral and polarization study.

.3 THEORETICAL EXPLANATIONS

2.3.1 Common X-ray and Radio Source vs Separate Source Models.

There are two somewhat different theoretical models which have been presented and analyzed in the literature to explain the correlated X-ray and microwave impulsive bursts. Both models attribute the microwave radiation to gyro-synchrotron emission by energetic electrons in regions above sunspots and attribute the hard X-rays to bremsstrahlung from regions of non-thermal electrons. They differ primarily in the location of these regions; Holt and Ramaty (1969) assume that in order to account for the close correlations between X-ray and microwave bursts the source regions for both bursts must coincide. On the other hand, Takakura and Kai (1966) and Takakura and Scalise Jr. (1970) postulate two separate regions in the sunspot associated magnetic field for the radio source (which in their model is a double source) and a third region for the X-ray source. The tight X-ray to radio correlations are attributed to a common energizing process injecting the high energy electrons into the sunspot magnetic field. The difference in the two Takakura papers lies in the fact that the later paper considers the detailed effects of non-uniformity in the $\bar{B}$ field within the radio source region itself.

These models are discussed to some extent by Kane and Donnelly (1971) and from this paper it is also evident that any models which are to be accepted must also account for the concurrent enhancement of ultraviolet radiation.

In reference to the double versus the single microwave source question, it is of interest to note that the original Takakura-Kai model was made before any observations of double sources were reported; it was deduced in an effort to account for the discrepancy between X-ray and microwave flux levels these authors as well as Peterson and Winckler (1959) felt would be inevitable in a single source model. The observation of a double source structure on a small percentage of bursts observed by the Japanese interferometer would certainly seem to support their theory; but since most sources have not explicitly exhibited the double structure it is still not settled whether in all the majority of cases there has indeed been a double source with one source too weak to observe or whether a true common single X-ray and radio source was in operation. In addition, no X-ray measurements of the X-ray source size and location have yet been obtained with the required precision. Our high time resolution measurements may help to settle this question if there were high time resolution X-ray measurements.

These two models of sources are used by their proposers to study the decay phase of the bursts starting from

initial assumed electron energy distributions and considering various electron energy loss mechanisms and the consequent changes in radio and X-radiation. None of the papers considers the electron injection or acceleration process itself or the evolving flux and polarization spectra during the impulsive increasing flux portion of the bursts.

2.3.2 Particle Acceleration Processes. In connection with the acceleration process, it is pointed out by Takakura and Scalise that in the Holt-Ramaty common source model continuous acceleration of electrons is necessary during the decay phase of the event since the collision decay of the electrons is faster than the decay time of the event. Also since electrons exceeding ~3 Mev energy have been detected in interplanetary space in connection with these bursts, these electrons should be emitting high frequency radio bursts of the order of a second in duration as they are being accelerated from ~750 Kev until they reach regions of smaller magnetic field and escape. These very short pulses have not been observed, since a time resolution of about 0.5 sec or better is needed, but conceivably could be observed in this proposed experiment.

The necessity for continuous acceleration and escape from the source region of electrons during the event is emphasized in the Kane and Donnelly paper, and also in Acton (1968). This latter paper also supports the possibility of a common region for the X-ray and microwave source electrons but requires they be in different energy ranges.

A further interesting aspect of the acceleration process is that a big boost has recently been given to the theory proposed by Petschek (1964) and modified by Friedman and Hamberger (1968) to explain solar flare particle ejection and the time behavior of the flare magnetic field structure by means of particle ejection at an X-type neutral point in a magnetic field in a process governed by diffusion assisted by MHD shock waves. Laboratory examination of the behavior of two colliding inverse pinches shows that the Petschek-Friedman-Hamberger model is basically what is operating in this experiment. [Bratenahl and Yeates (1970)]. Thus this is a starting point from which one could proceed to study the initial phases of the radio and X-ray bursts. It is of interest to note that in the laboratory experiments of Bratenahl and Yeates and others reported by Friedman and Hamberger which use parameters like those in solar flares (field strength, temperatures and densities) the magnetic energy

release is impulsive taking place on a micro-second scale.

The fact that hydromagnetic waves are associated in some way with the particle acceleration mechanism was also invoked qualitatively by Parks and Winckler (1969) to account for the observed 16 cycle modulation of the event they reported, and by Tanaka and Enome (1970) to account for the short time lag between excitation of the two radio sources in a double source. Finally we point out that a model something like the Petschek model for particle acceleration at a neutral point is invoked by Strauss and Papagiannis (1971) to explain the thermal X-ray emission during a small flare which was associated with a weak slow rise-and-fall burst observed at 2.8 GHz. In this case a common but very extended source region for the X-rays and microwaves was introduced.

2.3.3 Radiation Absorption Hypotheses and Computations; Their Polarization Effects. Returning to the two competing burst decay models, it is necessary to point out that in order to reconcile the observed flux levels in X-ray and in radio it was necessary for Holt and Ramaty to assume strong gyro-synchrotron self absorption of the radio emission. This is not needed for the Takakura and Kai model which assumes separate source locations and hence different electron densities and energy distributions for the two sources. Incidentally, an additional effective absorption mechanism at the low frequency end of the spectrum has recently been reported by O'Dell and Sartori (1970).

Additional strong suppression of the radio emission at the high frequency end is introduced by Holt and Ramaty via an hypothesized strong anisotropy in the electron distribution function which generates a strong directivity in the radiation at high radio frequencies. Takakura and Scalise directly counter this hypothesis on the grounds that one would then expect a wide range in the ratio of X-ray flux to radio flux from event to event, which is not in agreement with the observations.

One could counter their argument in turn by pointing out that there is probably a wide range of $\bar{B}$ field directions within the source (as discussed by Takakura and Scalise on the basis of the small statistical center to limb variations of the radio bursts). Then electron anisotropy could lower the net flux but this effect would tend to be the same from any source.

There are other differences in the two approaches. The Takakura papers do not take into account the ambient plasma effects on the radiation (Razin effect) nor the self absorption. On the other hand they treat thermal gyro-absorption by the ambient plasma which is an effect ignored by Holt and Ramaty who consider the ambient plasma to be cold.

The estimates made by Holt and Ramaty and earlier (to explain type IV bursts) by Ramaty and Lingenfelter (1967) of the effects of cold ambient plasma are probably poor. The Holt and Ramaty paper used theoretical results from Liemohn (1965) which are incorrect. That Liemohn's formulas lead to incorrect results has been observed by a Michigan student, Dennis Baker, in the course of his Ph.D. thesis work. Mr. Baker and Prof. Weil intend to check out how serious the errors are for parameters of interest to microwave impulsive bursts using Baker's computer programs. Independently, Trulsen and Fejer have also learned of the difficulty with Liemohn's results, as reported by them to the 1970 Spring URSI meeting (Commission 4). Trulsen and Fejer also point out that near the upper hybrid frequency, Cerenkov radiation is greatly reduced by thermal effects on the ambient plasma.

The Ramaty-Lingenfelter results are based on an extremely simplified model which neglects the magnetic anisotropy effects in the ambient plasma and so are doubtful. Baker and Weil intend to check out numerically the magnitude of the errors due to this simplification.

As a "warning" on this subject there is another very recent paper, Sakurai and Ogawa (1969), which purports to find not just the synchrotron or cyclotron power

radiated by spiraling electrons in ambient magneto-plasma, but the far zone fields. According to Weil and Baker, the equations for vector and scalar potentials which these authors "derive" and then solve are incorrect. These errors are not trivial in their effect, since evaluation of their final formulas under certain plasma conditions implies that there can be no radiation under these plasma conditions, whereas it is known by other theoretical means that there is indeed radiation.

The polarization shifts in sense with frequency are thought to be due to one or both of the following causes. For a single radio source the shift comes about because of the much stronger absorption coefficient for one sense of circular polarization than the other; particularly at the lower frequencies. This idea is found in all the theoretical papers although the postulated absorption mechanisms are different. In addition, Takakura and Scalise point out that, according to the model they adopt, there are always double radio sources, although one of the two may be negligibly weak so that the source appears to be a single source. For bursts originating at the limb the two sources could certainly not be resolved. In any case, each of the two regions in a double radio source will usually radiate opposite senses of polarization as confirmed by observation. When these are not resolved as separate sources, the

unbalance in source strengths may give an apparent reversal of polarization sense as opposed to the intrinsic reversal for each separate source.

According to the Takakura-Kai-Scalise (TKS) models in which absorption is due to thermal ambient plasma, the degree of polarization is strongly temperature dependent, as is the overall flux intensity. Multi-frequency polarization and flux measurements of simple sources will permit determination of the radial distribution of temperature in the medium between source and observer.

If the polarization and flux data is interpreted in the Holt-Ramaty model the measurements yield primarily data on the related quantities N, B and A, where N is the number density of (non-thermal) source electrons, A is the effective area of radiation projected normal to the earth-source line and B is a mean magnitude of magnetic induction in the source region.

At the lower radio frequencies, the Razin effect must be added to the TKS theory (as these authors acknowledge) and so the measurements will depend also on B and N, which will make an unambiguous interpretation of the data difficult. Conversely if warm surrounding plasma is considered in the Holt-Ramaty model, its temperature will then be a factor influencing the results as well as N, B, and A.

2.4 OTHER USES OF RAO.

2.4.1 85-foot Radio Telescope. The University of Michigan Radio Astronomy Observatory is supported under National Science Foundation Grant GP-21349. Under this grant, research has been continued in the following areas: measurement of polarization and flux density of variable radio sources, and using the observations to refine the models of variable radio sources; a sky survey at λ3.75 cm which has shown an excess of extra-galactic sources over that predicted by lower frequency surveys; measurement of radio sources to extend their spectrum to λ3.75 cm; measurement of hydrogen and helium recombination lines and possible molecular emission lines in the frequency range of 8.5 to 9.5 GHz; measurement of flux density at different wavelenths from Venus, Mars, Jupiter, Saturn, Uranus and Neptune; a search for fast period variable sources.

In addition, work continues to improve the sensitivity and stability of the radiometers, and to improve auto reduction and data processing techniques.

A proposal has been submitted to the National Science Foundation for the support of the University

of Michigan Radio Astronomy Observatory for the period August 15, 1971 to August 14, 1972. The proposed objective for the coming period will include part of the following programs (most observations made at wavelengths of 7.5, 3.8, and 1.3 cm):

1. Measure the variation of polarization and flux density of non-thermal sources, quasars and Seyfert galaxies and radio galaxies.

2. Continue the measurement of flux densities of radio sources, both those reported at longer wavelengths and those found here at λ3.75 cm wavelength.

3. Continue a sky survey search for new sources.

4. Continue a program to search for variable radio sources that exhibit rapid intensity variations.

5. Measure the flux density at different wavelengths from Venus, Mars, Jupiter, Saturn, Uranus, and Neptune, as time permits.

6. Measure the intensities and line widths of Hydrogen and Helium recombination lines in HII regions and search for molecular line emissions in the frequency range of 8.5 to 9.5 GHz.

7. Continue to improve the sensitivity and stability of the radiometers.

8. Continue some theoretical and numerical analysis of data reduction and improve data processing techniques.

This proposal requested funds to support graduate students and staff, to maintain the radio telescope, process the data, and improve the equipment. Professor F. T. Haddock will continue as director of the Radio Astronomy Observatory. He will be assisted by Professor H. D. Aller in astronomical research and by Dr. T. V. Seling who is responsible for the instrumentation, operation and maintenance of the facility. Two engineers and two technicians will maintain and help operate the facility. Members of the Radio Astronomy Staff and graduate students will collect and analyze data from the radio telescope. There are five graduate students using the telescope at the present time.

2.4.2 28-foot Radio Telescope. The 28-foot Radio Telescope and equipment house is presently available for use with the proposed SMS.

2.4.3 XDS-930 Computer Facility. The computer facility, described in Section 7.2, is presently being used to process data from the low-frequency radio astronomy experiment aboard the OGO-V satellite under NASA/GSFC Contract NAS 5-9099. NASA/GSFC anticipates extending

this contract to 31 March 1972. The present computer usage by the OGO-V program is approximately 50 hours per week.

The low-frequency radio astronomy experiment aboard the IMP-I satellite will also use the computer facility for data processing. The IMP-I satellite was launched on 13 March 1971 and is collecting good data. NASA/GSFC Contract NAS5-11174 for the data reduction and analysis is expected to continue through March 1973. The estimated computer usage for this program is 20 hours per week.

3. ENGINEERING PLAN

3.1 DESIGN OBJECTIVES

The prime objective of this study is to determine if it is feasible to design a system which will fulfill the scientific goals, set forth in Section 2 above, at a reasonable cost. The feasibility was established early in the design study thereby allowing more effort to be placed on secondary goals. These secondary goals are numerous and, taken as a whole, are an attempt to optimize the system design. These secondary goals, listed briefly below, are discussed fully throughout this report.

Secondary Goals

(a) Design and partition the receiver such that it could be mounted on either the 28-ft or the 85-ft dish.

(b) Expansion capability so designed that little if any, of the initial system design will have to be discarded.

(c) Maximum reliability and minimum maintenance.

(d) High degree of flexibility of operational modes from full automatic to manual.

(e) Optional automatic flare alert system for minimum operator intervention and minimum data collection during non-flare periods.

(f) Simple programming language such that the operator and/or scientist can easily generate new operational modes

(g) System check-out, automatic or on command, for verification of proper operational mode and for malfunction diagnostics.

3.2 SYSTEM DESCRIPTION AND BLOCK DIAGRAM

The proposed Solar Microwave Spectrograph (SMS) basically consists of an antenna, a receiver, a data handling subsystem and a central controller as shown in Figure 1. The antenna is the 28-foot radio telescope located at the UM/RAO with a broadband (2-8 GHz) antenna feed. Microwave hardware is provided to select orthogonal linear polarizations or orthogonal circularly polarized signals and to split the received signals into the octave frequency bands of 2-4 GHz and 4-8 GHz. Two independent receivers (one for each octave) amplify the signals, divide the octave band into 10 frequency channels in the directional filters, and logarithmically detect the output of each of the filter channels. The data handling subsystem, shown in the simplified block diagram of Figure 1, sequentially samples the detected output of the twenty frequency channels with a multiplexer, converts the analog samples to digital in the A/D converter, labels and formats the data in a data formatter, records the data on magnetic tape, and processes it at the existing XDS 930 computer facility for analysis. The central

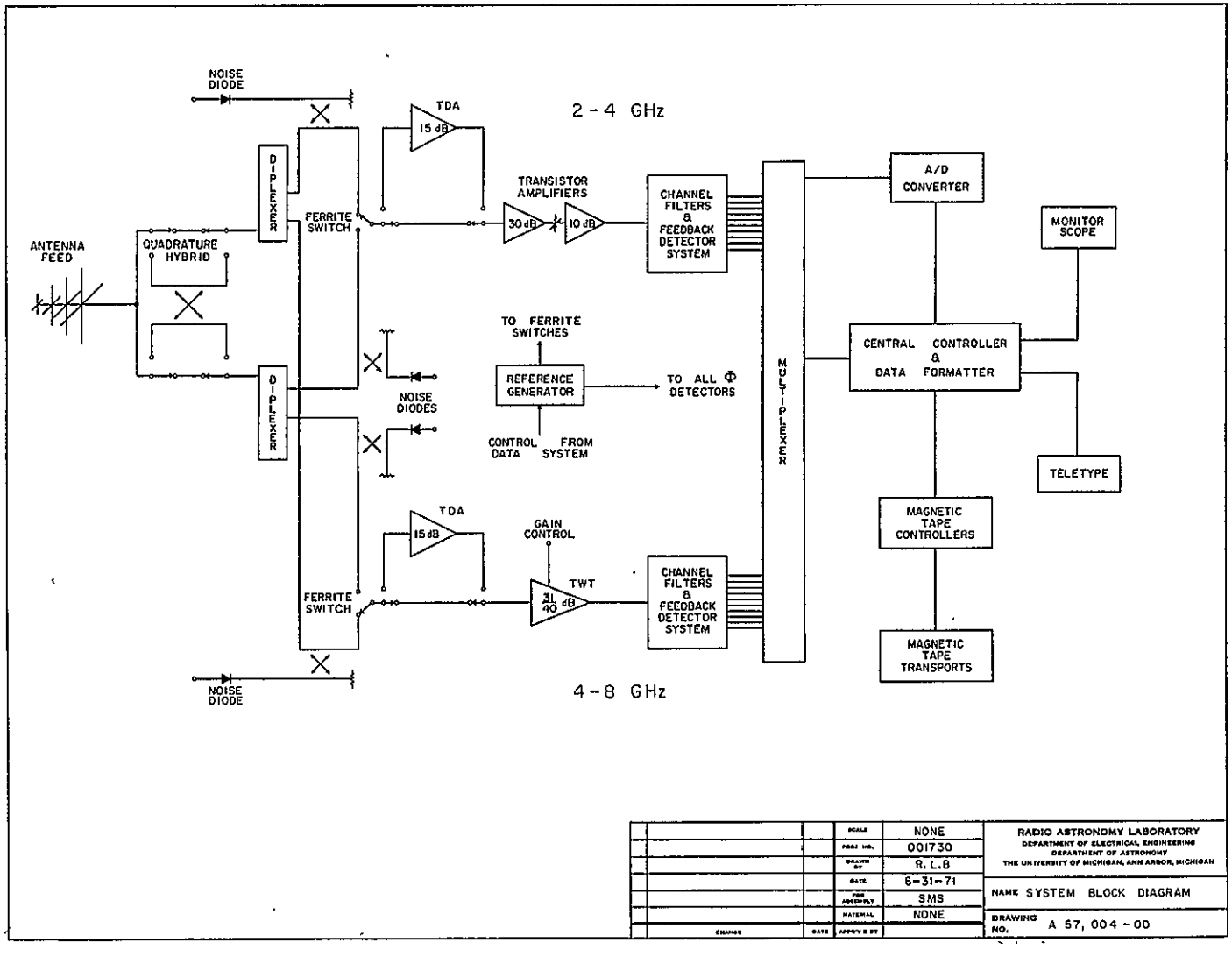

Figure 1. System Block Diagram

controller is the subsystem of the SMS instrumentation which provides the timing,.the sequence of commands necessary for the particular mode of operation, and preparation of data for the real-time display. In addition to the basic system described above, noise sources are provided for periodic system calibration, a cosmic channel is provided for antenna calibration using radio sources,a monitor scope is provided for real-time display of the radiometer output, and the central controller is used for system functional checks and malfunction diagnostics.

The complete system specifications for the Solar Microwave Spectrograph are contained in Table 2 below.

The SMS system has the high degree of flexibility of operational modes required by the scientific objectives of the instrument. This flexibility makes it very difficult to set down a specification which is meaningful and which conveys the capabilities of the SMS. The presently envisioned operational modes are presented below in an effort to convey the information necessary to fully appreciate the capabilities of the SMS system.

Table 2 SMS System Specifications

	28-foot	85-foot
ANTENNA AND FEED		
Beam width (2-8 GHz)	73' - 18'	24' - 6'
Side Lobe Level (2-8 GHz)	< -20 dB	< -20 dB
Pointing Accuracy (2-8 GHz)	2'	1/2'
RECEIVER		
Dynamic Range Available		
Solar Observations 2-4 GHz	29 dB	33 dB
4-8 GHz	29 dB	35 dB
Frequency Range	2-8 GHz	
Frequency Resolution	7% (10 channels/octave)	
Polarization	Circular or linear	
Polarization Switch		
Settling Time	≈0.1 milliseconds	
Time Resolution		
Solar Observations	0.1 milliseconds	
Radio Source Observations	0.1 second	
Receiver Noise Temperature		
Solar Observations (ex solar noise)	2700°K	
Radio Source Observations	700°K	
RMS Receiver Fluctuation Noise		
Solar Observations ($\tau=1\times10^{-4}$s)	<1/2% of signal	
Radio Source Observations (τ=10s)	0.026°K @2 GHz 0.013°K @8 GHz	

Table 2 SMS System Specifications (Continued)

DATA HANDLING SUBSYSTEM

ΔT/T Resolution Due Quantization for 40dB Dynamic Range	<1%
Time Resolution	<5μsec.
Sampling Interval (programmable)	≥20μsec.
Data Throughput Rate	
Express Mode	18,000 samples/sec
Normal Mode	9000 samples/sec
Time Accuracy-Relative (Subsystem clock stability)	10^{-6}
Time Accuracy - Absolute (Using WWV input)	<.1 sec.

a) Antenna

1) Automatic tracking of the sun
2) Manual pointing

b) Polarization

1) Select either component of linear or circular
2) Switch between linear components or between circular components at up to 1 KHz rate

c) Receiver

1) Solar observations
2) Radio source observations for system calibration

d) Data Handling Subsystem

1) Select number and sequence of frequency channels to be sampled.
2) Select sampling rate--up to 18,000 samples/sec (900/sec full 2-8 GHz frequency scans)
3) Select automatic flare mode or manual operation
4) Select automatic flare mode selection criteria
5) Select number of samples to be averaged during non-flare periods when in automatic flare mode
6) Select number of samples to be averaged during flare or radio source observations.

e) Central Controller

1) Select calibration mode
2) Select real-time display format
3) Select system test mode

As an example, consider the following normal mode of operation: The antenna automatically tracks the sun all

day. When there is no flare (on the basis of the automatic flare mode selection criteria), the 20 frequency channels will be sampled once every 2.2 msec (full 2-8 GHz frequency scan), the controller will direct Tape Recorder No. 1 to record all of the samples. Simultaneously, the data formatter will average 100 of these sets (20 frequency channel samples) and direct Tape Recorder No. 2 to record the averaged data. (A full day's averaged data can be recorded without changing tape.) If a flare is not detected during the recording of the tape on Recorder No. 1, the tape is rewound and recorded over again. Meanwhile, Recorder No. 3 has been substituted for Recorder No. 1 so that no data is lost. If a flare had occurred during the recording of data on Recorder No. 1, an alarm would have sounded to alert attendant personnel, and the tape on Recorder No. 1 would be removed for later analysis. The number of tapes removed for analysis is related to the flare duration. The central controller keeps track of which tapes contain flare data and will not reuse those tapes. If all tape recorders contain flare data, further flare data will not be recorded until the tapes containing the flare data are replaced. The data tapes are transported to the SDS-930 computer for data reduction.

3.3 ANTENNA AND FEED

The antenna system planned for use with this experiment is the 28-foot paraboloid at the University of Michigan Radio Astronomy Observatory. A feed system covering the 2-8 GHz band will be split into two octaves (2-4 GHz and 4-8 GHz) and provide outputs for orthogonal polarizations, either linear or circular polarization.

3.3.1 Antenna. The 28-foot parabolic reflector has an F/d ratio of 0.423 and a surface accuracy that makes it useable to a wavelength of 3 cm. A visual inspection of the surface of the 28-foot telescope shows it to be in good condition, with only a few small cracks in the fiber glass surface near the edge. Although we do not have the exact specifications of the surface at present, we see no reason for it to have changed from the original condition which was usable to 3 cm. A 100 to 600 megahertz feed system is mounted on the antenna and must be removed to install the 2-8 GHz feed system. Most of the cabling from the apex to the house will have to be replaced.

The antenna is completely operable, but the drive systems need to be inspected, cleaned, lubricated, and any necessary repairs made.

It was noted on an average day that there was approximately 4 min of arc backlash in the declination drive, and 15 sec of time in the hour angle drive. This was observed at the synchro readouts on the console. With this antenna, it is possible to reduce this backlash be adding counterweight.

The equipment house is located near the 28-foot antenna and houses the antenna controls and associated receiving equipment. The building is air-conditioned and all facilities in this building are in good working condition.

3.3.2 Antenna Feed. Three basic antenna feeds were considered for this application: the log-periodic dipole, the sleeve dipole, and the ridged horn. Only two of these antenna appear suitable for this application, the sleeve dipole and the ridged horn. The log periodic dipole has the disadvantage that its phase center moves axially with frequency, and over the 4:1 band planned for the system, defocussing of the feed would occur at the longer wave lengths. Another disadvantage of this antenna is that a diplexer is required to separate the two octave bands.

The antenna feed system proposed for this application is a combination of the ridged horn and sleeve dipole. For the 4-8 GHz band, a ridged horn would be used with orthogonal linear polarized outputs. For the 2-4 GHz band an array of two sleeve dipoles over a ground plane would be used. Two arrays at right angles would be used to provide the orthogonal linear polarizations.

The complete feed system would consist of the ridged horn surrounded by four sleeve dipoles arranged in a square around the ridged horn with a ground plane. There are two orthogonal linearly polarized outputs for each octave band, which can be combined in broad band quadrature hybrids in the receiver to provide orthogonal circular polarization if desired. A similar feed system is used on the University of Illinois 150-foot antenna for two frequency operation.

3.3.3 Antenna System Characteristics. The overall antenna characteristics with the proposed feed system are summarized below.

Frequency Range	2-8 GHz
Polarization	Selectable orthogonal linear or circular
Half-Power Antenna Beamwidth	Varies with frequency from approximately 24 minutes at 8 GHz to 96 minutes at 2 GHz
Sidelobe Level	<-20 dB
Antenna Efficiency	Approximately 50%
Unwanted Polarization	Down 15 dB or more
VSWR	<2:1

3.4 RADIOMETERS

A proposed receiving system configuration is presented for the measurement of solar bursts over a two octave range from 2 to 8 GHz. The system uses multiple filter channels of constant percentage bandwidth spaced to provide continuous coverage of the frequency range of the receiver. The frequency resolution, i.e. number of channels per octave, is primarily determined by the characteristics of the channel filters.

Directional filters appear to be the most applicable type of branching filters for this application. For ease of fabrication, the filter is limited to one tuned circuit, which limits the 3 dB bandwidth to about a minimum of 7%. This percentage bandwidth gives 10

channels per octave, or a total of 20 for the full frequency range of 2-8 GHz. The data recording system is capable of time resolution of 1.1 milliseconds (express mode) with this number of channels. Noise in the receiver is on the order of 1/2% of the received signal or less as determined in Appendix A. Using these considerations, the basic receiver characteristics are:

Frequency Range	2-8 GHz
Frequency Resolution	7% (10 channels/octave)
Time Resolution	1.1 ms. for 20 channels
RMS Receiver Fluctuation Noise ($\tau = 1 \times 10^{-4}$ sec)	<1/2% of received signal

3.4.1 Basic Receiver. In this application, the primary noise in the system is due to the sun itself, and a DC radiometer system is proposed. A comparison system would have no advantage since noise due to the effect of gain variations on the receiver internal noise is negligible. The minimum input signal for the 28 foot antenna varies from about 4×10^4 K(2×10^5 for the 85-foot) at 2 GHz to about 2×10^4 K for both antennas at 8 GHz. Since this input noise is not sufficiently large to use detectors directly, preamplification is required prior to detection. The dynamic range of the signal for the 85-foot antenna varies from about 150:1 (22 dB) at 2 GHz to approximately 1000:1 (31 dB) at 8 GHz.

In the middle of the frequency range (4 GHz), the dynamic range is 250:1 (24 dB), as derived in Appendix B. The dynamic range for the 28-foot antenna is less than for the 85-foot as derived in Appendices C and D. Since this range of signals is rather large, some means of compressing the output signal of the system, preferable logarithmically, is desirable.

Based on these requirements, a concept using a closed-loop feedback system is proposed. This system uses a variable attenuator preceding the detector for each channel, controlled by a feedback system to maintain the detector output voltage constant. The output parameter of the system is the current (or voltage) used to control the attenuator. Ideally, the attenuation would be a logarithmic function of the control current or voltage (or a similar function that would provide adequate compression of the signal) that could be corrected in the data reduction to provide a suitable output or display such as linear or logarithmic.

The basic block diagram of the proposed system is shown in Figure 1. There are two inputs to the receiver which can be used for orthogonal polarizations.

These inputs are obtained from the antenna feed system which produces orthogonal linear polarized signals or, using a quadrature hybrid, orthogonal circularly polarized signals. These inputs are split into two octave bands, 2-4 GHz and 4-8 GHz by diplexers. The outputs of the diplexers are then directed to the appropriate receiver channels. Octave bandwidth RF switches at the input of each channel permit selection of either polarized signal, or by rapid switching, time duplexing of the inputs can be obtained. Calibration is provided by avalanche diode noise sources that have noise temperatures on the same order of the quiet sun.

The two receiving channels are basically the same. Octave band RF amplifiers are used to provide sufficient amplification of the signal to make the noise of the detector system negligible, followed by a 10-channel filter. Each output channel then uses a feedback detector system which provides compression of the received signals.

Operating in the polarization switching mode, the switching rate is synchronized with the data acquisition system, and the data reduction can provide the sum and the difference signal, as well

as the individual power of the two inputs.

3.4.2 Wide Band Amplifiers. Transistor Amplifiers (TA), Tunnel Diode Amplifiers (TDA), and Traveling Wave Tube amplifiers (TWT are available in this frequency range for the wideband amplifier. TA's are small, relatively low noise (<10 dB NF at 4 GHz), have modest power requirements, and relatively high power output (+10 dBm for 1 dB gain compression), but are only available for the 2-4 GHz octave. TDAs are available for the full frequency range, but have rather low output powers for 1 dB gain compression (approximately -10 dBm), which would limit their dynamic range to about 20 dB. TWTs have the disadvantage of limited life and a higher output power consumption, but have considerably higher output power capabilities (+7 dBm for 1 dB gain compression) than TDAs. Therefore, it is proposed to use a TA in the 2-4 GHz octave and a TWT for the 4-8 GHz octave. Using available amplifiers, typical characteristics are:

2-4 GHz Transistor Amplifier:

Noise Figure	10 dB max
Output Power at 1 dB gain Compression	+10 dBm min
Gain Flatness	±1 dB at 40 dB gain
Available Gain	Up to about 50 dB in 10 dB increments

4-8 GHz Travelling Wave Tube:

Noise Figure	8 dB max
Output Power at 1 dB Gain Compression	+7 dBm
Gain Flatness	±1 dB at 40 dB gain
Available Gain	Approx. 40 dB max for one TWT

In the 2-4 GHz octave, using a gain of 40 dB, the dynamic range for 1 dB gain compression would be 29 dB, about 11 dB greater than the expected range of input signals. The range of output power would be from -18 dBm for the quiet sun to an expected maximum of -1 dBm. In the 4-8 GHz octave, using a gain of 34 dB, the dynamic range for 1 dB gain compression would be 29 dB, about 10 dB greater than the expected range. The range of output power would be from -22 dBm for the quiet sun to a maximum of -3 dBm. For use on the 85-foot radio telescope, the gains can be adjusted to provide dynamic ranges with a margin of 10 dB in the 2-4 GHz octave and 7 dB in the 4-8 GHz octave.

3.4.3 Detector System. The detector system consists of a filter for each channel followed by a variable attenuator and detector. The detector output voltage is compared with a reference voltage and the error signal is used to control the attenuator to maintain the detector voltage constant. The control

signal to the attenuator is used as the system output. Figure 2 is a block diagram of the detector system.

The critical element in this system is the controllable attenuator. This attenuator must be a non-linear function of the control voltage (or current) to produce compression of the dynamic range of the signal with a function that is either logarithmic or close to a logarithmic function so that data reduction can convert the signal to logarithmic or linear form easily. A PIN diode attenuator most nearly meets these requirements.

The PIN diode is a semiconductor diode that has an RF resistance that is a power-law function of the DC current through the diode. Typically, the resistance, $R = KI^{-x}$, where K might typically be on the order of 13 and $x = 0.86$. Used as a shunt element in a transmission line, the attenuation varies as a function of current in the form of $A(dB) = C \log (Z_o K I)$.

In practice, the PIN attenuator has a logarithmic attenuation as a power function of the DC current through the diode. A typical PIN diode attenuator

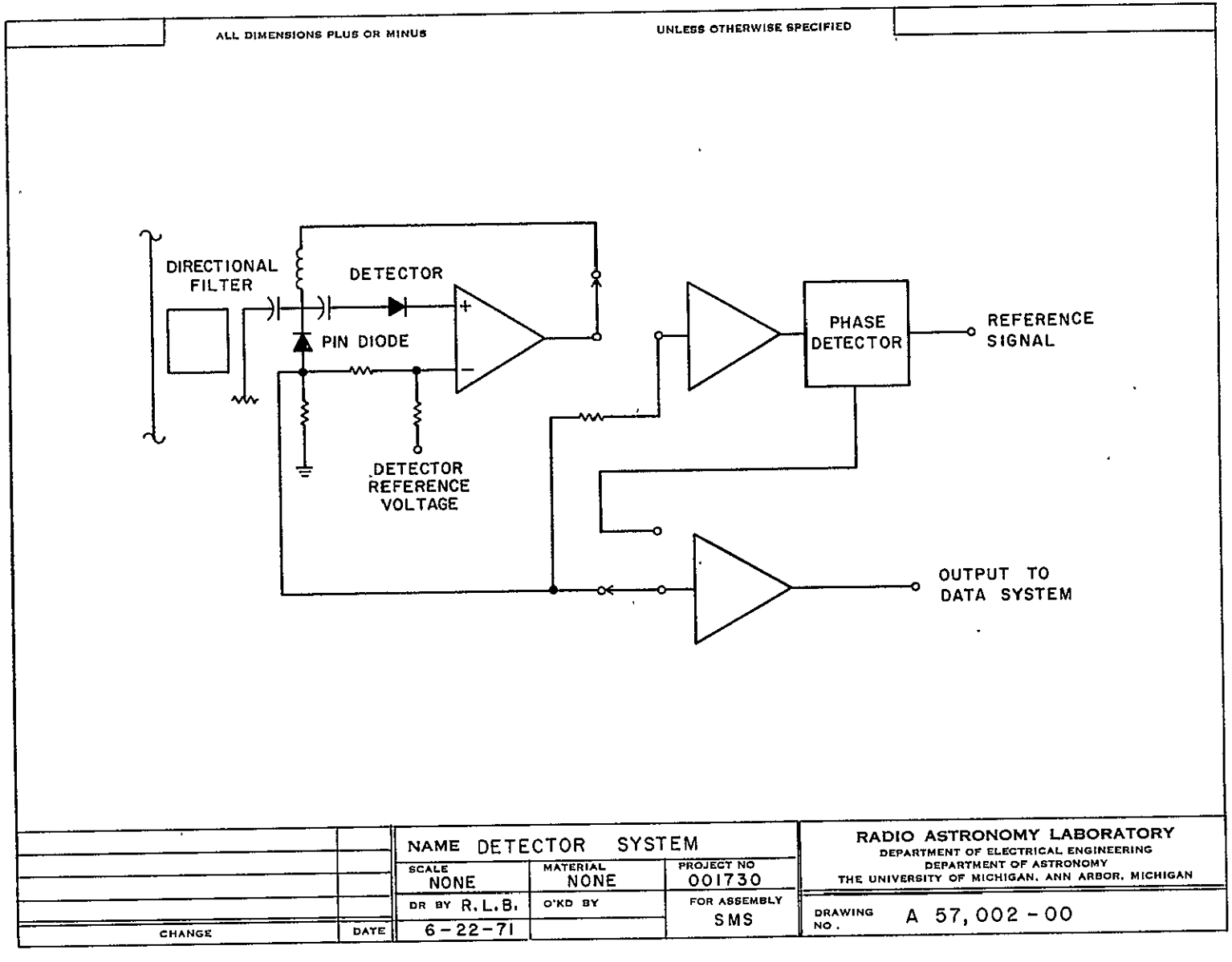

Figure 2. Detector System Block Diagram

(Sylvania DSJ-6112) has the relation between attenuation, A, and current

$$A(dB) = 19\ I^{0.643}$$

where I is the current through the diode in milliamps. Thus, since the attenuation is proportional to the input power or temperature,

$$I^{0.643} = B \log (T_S + \Delta T_S)$$

Alternately, non-linear shaping of the attenuation vs. current function can be used such that the attenuation in dB is directly proportional to the applied voltage. This is generally accomplished with diode shaping networks and is therefore a piece-wise linear approximation to the log function. A typical "linear" attenuator has errors on the order of ±1/4 dB per 10 dB of attenuation.

The range of a single PIN diode attenuator is on the order of 20 dB, but the constant power-law relationship only holds over a range of about 10 dB without compensation. Thus for this application, an attenuator using 4 diodes would be necessary.

The remainder of the detector system uses operational amplifiers to drive the attenuator, and the output voltage or current is used as a measure of the attenuation and hence the input power or temperature.

3.4.4 Radiometer and System Testing. Radiometer and system testing requires the generation of broadband high level noise or the use of a discrete easily tuneable CW oscillator. Secondly, the means of injecting the test signal into the system is also somewhat of a problem. Ideally the signal should be transmitted into the system from an antenna located at the vertex of the parabola. A second choice would be to inject the signal into the system through a directional coupler. The last choice would be to switch the input of the receiver from the antenna to the calibration source. The noise source is proposed for this system because it closely simulates the received signal, requires only amplitude control by the system controller (CW signal generators also require frequency control), and allows the calibration to be completed in a shorter time period since it is done by octaves instead of discrete frequencies.

The requirements for a broadband noise source are a minimum power spectral density of -64 dBm/MHz and an octave bandwidth. This corresponds to the expected input level to the receiver for a major solar burst. An output power spectral density of -54 dBm/MHz is desirable in order to test the system

over its full dynamic range. Noise sources of this level are not generally available in this frequency range, and in general require an amplifier to raise the output of a noise generator to the desired power level.

For the 2-4 GHz octave, a combination of an avalanche diode noise source and a transistor amplifier can be used as a high-level noise generator. Avalanche diode noise generators generate noise on the order of 3×10^5 °K, which is a power spectral density of -84 dBm/MHz. If this noise is amplified with a gain of 30 dB, then the output power spectral density is -54 dBm/MHz. The total noise power output of the amplifier is -21 dBm. The variation of the output noise over the band will typically be on the order of 2-3 dB. A PIN diode attenuator on the output can be used to provide an electrically variable attenuator so that the noise output can be easily controlled by an external voltage command. An AGC system would be used to control the noise output, and the AGC reference voltage would be used as the command voltage.

For the 4-8 GHz octave, traveling-wave-tube amplifiers are available that can be used as noise generators.

For example, the MEC MJ2207E has the following characteristics.

Frequency Range	4-8 GHz
Gain	30 dB Min.
Noise Figure	30 dB Max.

Assuming a noise figure of 30 dB and a gain of 30 dB, the characteristics of this generator would be essentially the same as the 2-4 GHz noise generator. Gain control of the TWT gain would be easily accomplished by varying the control grid voltage. Typically, the gain control is 1 dB/volt. Again, an AGC system would be used to control the noise output, and the AGC reference voltage would be used as the command voltage input.

Block diagrams of the systems are shown below. The amplitude and frequency control voltages could be furnished from the system controller through D/A converters.

3.4.5 Antenna Calibration. To calibrate the antenna system, it is necessary to use radio sources that are small compared to the half-power beamwidth of the antenna. Radio sources suitable for calibration are considerably weaker than the sun. Therefore, additional gain is needed in the receiver to make the

detector noise negligible. Also, the receiver noise should be made as small as practical so that an adequate signal-to-noise ratio can be obtained without excessively long integration times.

To meet these requirements, germanium TDA's are proposed as preamplifiers preceding the main TA or TWT. These amplifiers would be switched in or out of the RF amplifier chain as needed. The RF gain in the receiver would be increased to approximately 55 dB by the addition of these amplifiers and an increase in gain of the main wideband amplifier to about 40 dB. This would be accomplished in the 2-4 GHz octave by adding a transistor amplifier with approximately 10 dB gain and in the 4-8 GHz octave by grid control of the TWT.

Since the signals from radio sources other than the sun are in general small compared to the receiver noise, the receiver must be operated as a comparison radiometer to eliminate gain fluctuation noise. The dynamic range of the receiver output for radio sources other than the sun is in general less than 1.5:1 and the feedback detector system is not necessary or desirable. Therefore, a conventional audio amplifier and phase detector are used to recover the signals. Data acquisition for

radio sources is at a relatively slow rate, on the order of 1-10 seconds, and no additional requirements are placed on the data acquisition system.

The overall characteristics for radio source work are listed below.

Frequency Range	2-8 GHz
Frequency Resolution	7% (10 channels/octave
Time Resolution	<0.1 second
Receiver Noise Temperature	<700 K
RMS Receiver Fluctuation Noise	0.026 K at 2 GHz
($\tau = 10^{s}$)	0.013 K at 8 GHz

This sensitivity is sufficient to permit measurement of the antenna pattern and sidelobe structure in order to evaluate the antenna performance over the expected range of declination and hour angle.

The detector system is capable of operating as a feedback system for solar work, or as a conventional switched system with phase-sensitive detectors. All switches in the RF portion of the receiver are mechanical coaxial types except the comparison switches at the receiver inputs. These switches are octave bandwidth ferrite switches to permit rapid switching in the comparison mode of operation.

3.5 DATA PROCESSING AND STORAGE

The objectives of the experiment require that the data acquisition system be capable of sampling, digitizing, and recording data at a rate approaching one sample every 100 μsec, or 10,000 samples per second. A few key considerations govern the design of such a system:

1. Multiplexing and analog-to-digital conversion at this rate present no problems. Inexpensive units are available which will perform these functions in less than 20 μsec.

2. Standard computer-compatible magnetic tape seems to be the only reasonable choice for the data recording medium. It is the only readily available medium that can handle the data rate and store sufficient data in a readily transportable form.

3. Continuous recording at the high data rate is very costly, producing as many as 50 magnetic tapes per day. This fact, together with the intermittent nature of the solar events being sought, indicates that some automatic selection process should be interposed, so that data is preserved for further processing only if there is some indication that solar activity is present.

4. Any reasonable data formatter can support the required data rate if it has very little to do besides the input/output operations. If direct access channels are provided to relieve the program of the burden of input/output, a typical data formatter and central controller can perform simultaneous processing equivalent to several operations per data word.

In the light of these considerations, the proposed data acquisition system is designed to be capable of operating in the basic mode where all data samples are recorded on a high-resolution output tape. Simultaneously, a solar activity detection test is applied to the data. If, during the recording of a tape, there is no indication of solar activity, the data are not preserved, the tape is rewound, and new data written on it. By recording all samples and preserving only those which possibly represent solar activity, we have the option of also preserving data for the period before activity was detected.

The system is also capable of simultaneously generating a low resolution data tape, where samples are averaged in time to condense the data so that a single tape will contain an entire day's data. The time resolution of this tape will be of the order of a few tenths of a second, and this tape will be preserved whether activity is detected or not.

3.5.1 System Description. The proposed data acquisition system as shown in Figure 3 consists of a central controller with a multiplexer (MX) and analog-to-digital converter (ADC), four magnetic tape transports with two controllers, a monitor scope, a master

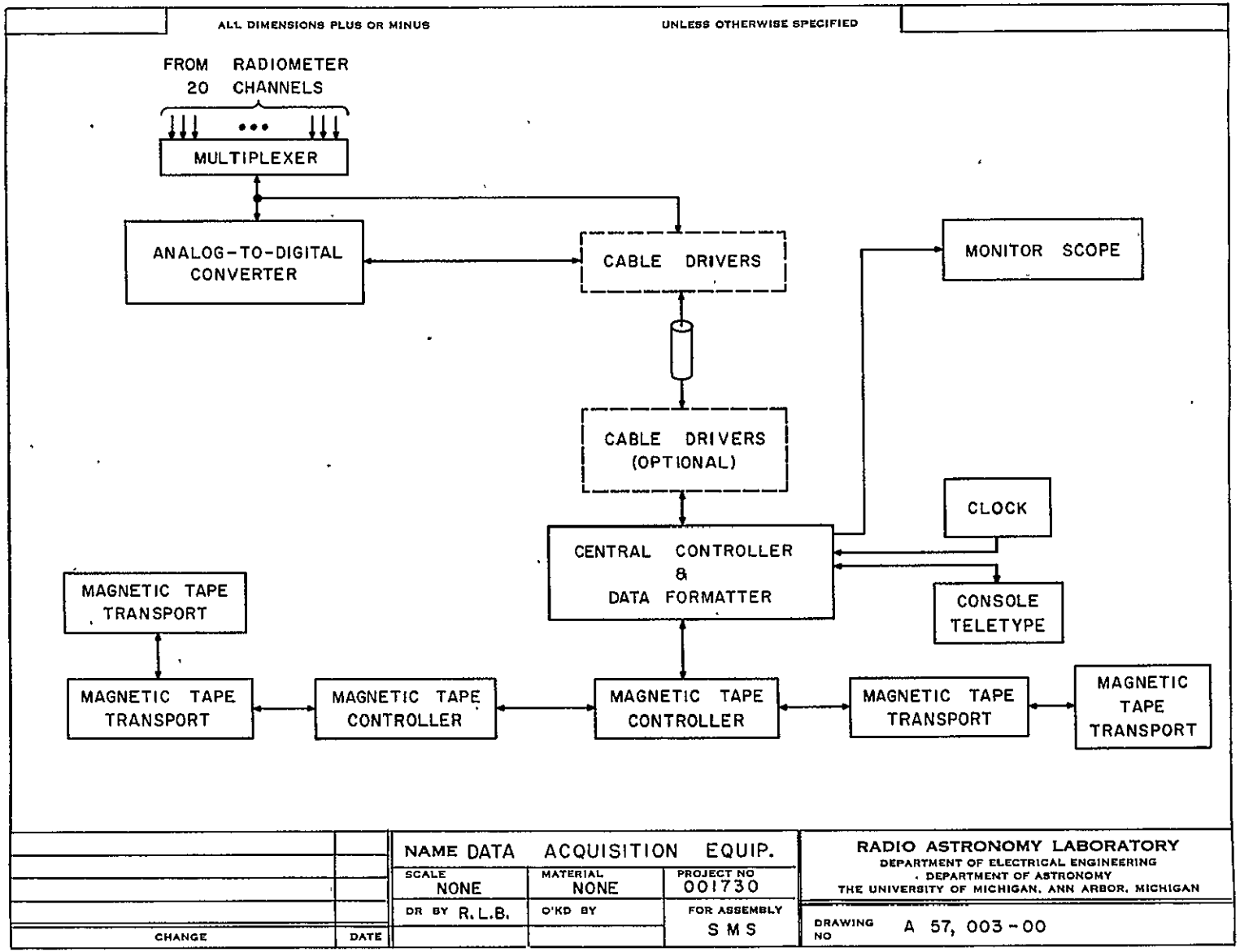

Figure 3. Block Diagram - Data Acquisition Equipment

timer, and a console teletype. For planning purposes, the central controller and data formatter are assumed to be made up of standard off-the-shelf hardware produced by several manufacturers.

Central Controller. The central controller should be capable of controlling the MX and ADC while recording data simultaneously on two magnetic tapes and performing simple formatting and processing functions. A 12-bit machine with 8K of core memory seems to be appropriate, but 16-bit machines should not be ruled out at this point. Direct memory access channels or other means of relieving the main program of a part of the I/O task may be required.

Multiplexer and Analog-to-Digital Converter. The analog input portion of the data acquisition system consists of a multiplexer (MX) and an analog-to-digital converter (ADC) with the following characteristics:

Precision:	10 to 12 bits
Range	0 to +10 volts
Conversion Time:	Less than 30 μsec total time per conversion
No. of Channels:	32, with the capability of expansion to 128.

In the normal mode of operation, the 20 channels which carry radiometer information will be sampled regularly, in a sequence, while the remaining channels, which carry housekeeping and reference information, will be sampled less often, and in an irregular sequence.

A precision of 10 bits is somewhat marginal, as shown in Appendix E, and can be permitted only in conjunction with some kind of gain switching to increase the effective precision in the lower portion of the range.

Magnetic Tape Units. The magnetic tape sub-system must be capable of supporting the normal mode of operation, where data samples are gathered at a rate approaching 10,000 samples per second, merged with housekeeping and reference data, formatted into convenient sized records, and written on a tape. Occasionally a condensed data record must be written on another tape, without interrupting the flow of direct samples. A further desirable feature is to have on-line storage capacity for direct samples that is equivalent to at least three magnetic tapes. Various tape configurations will meet these requirements, but the following configuration seems to be the least expensive.

Four tape transports are required, with two tape controllers, so that two tapes may be written on at once. Normally, the tape units will be distributed with two on each controller, but each controller must be capable of handling at least four tape units, to provide the capability of operating all tapes on one controller, and also the capability of expanding the number of tapes.

Format:	Standard 7-track, 556 char/in.
Speed:	45 in/sec or greater.
Fast Rewind:	Less than 5 min.
Start-Stop Time:	Sufficiently fast to maintain the data rate.

Less than 10 msec total start-stop time is probably required.

Monitor Scope. A monitor scope is provided so that the operation of the entire instrument may be checked periodically. The monitor can display signal strength as a function of time or frequency, and can display a single trace or multiple trace. Probably the most useful form of the display will be a real time display of radiometer output as a function of frequency, which will form a dynamic spectrum. Interference or malfunction in one or more channels would be quite conspicuous in this

presentation. The display can also be used to "play back" data which has been recorded on tape, giving the capability to check the performance of the tape recorders, and to review data which was previously collected.

The proposed implementation for the monitor scope is an inexpensive controller driven display, driven by the data acquisition system. A storage screen CRT is proposed, so that the system will not be burdened with the task of refreshing the screen. The frequency with which the system can update the display will depend upon the data rate at which the data acquisition system is operating. In the express mode, it may not be possible to operate the display at all, but in the test mode, the full capability of the display should be available.

The magnitude of the programming task which is required to implement the display depends heavily upon the software which is available with the display. This factor must be taken into account in selecting the equipment.

A secondary use of the controller driven display is as an alpha-numeric output device for presenting messages to the system operator.

Master Timer. It may be necessary to determine the Universal Time at which each data sample was taken to an absolute accuracy of about ±1 ms. The mastertimer, incorporated into the data acquisition subsystem, can provide an indicated time, accurate to better than one second, and timing signals based upon WWV by means of which the indicated time can be corrected to attain an accuracy approaching ±1 ms.

The indicated time is generated by a crystal oscillator which is counted down partly by hardware counters and partly in the data acquisition system. This count controls the sequencing of the multiplexer, and the strobing of the analog-to-digital converter, and the time words which are inserted into the data records. Indicated time is checked and set manually.

The error in the indicated time is determined by periodically feeding time signals derived from a WWV receiver into the data acquisition subsystem which records sufficient information in a special "time check record" on the data tape to permit a

time correction to be derived when the data are reduced. The correction would be derived at the beginning of each data tape, and more often if the data were being sampled at a slow rate, so that a long time would be required to fill a tape.

3.5.2 Modes of Operation. Three modes of operation are postulated at present, and others may be proposed later, even after the system is operational. The three modes to be described here are: (1) Normal, (2) Express, and (3) Test.

Normal Mode. This is the mode in which the system would be expected to operate most of the time. In this mode, the rate at which the radiometer outputs are sampled may be set at any rate up to a maximum of about 2.2 ms/sample. All samples are digitized and recorded on the "high resolution" magnetic tape. Simultaneously, an averaging operation is performed to condense the data, and the resulting summary data are recorded on the "low resolution" tape. Also, a simple test is applied to the radiometer output to determine if evidence of solar activity is present. If, during the entire period

while high-resolution data are being recorded on a magnetic tape, there is no evidence of solar activity, the tape will be rewound and later written over, destroying the high-resolution data for that period. The condensed data, however, will be saved. If evidence of activity is found during the recording of a tape, the controller will signal the operator to come and dismount that tape, saving the high-resolution data. This procedure makes it possible to always save about a half-tape of data that were recorded before there was detectable evidence of activity.

Express Mode. The express mode is designed to achieve the maximum possible data rate, at the cost of an inconvenient format for later processing, and sacrificing the recording of condensed data. Maximum data rate is achieved by writing on two tapes at once, splitting the data either by recording half the radiometer channels on each tape, or recording half the time samples on each tape. Either way, an additional burden is imposed on the later processing operations, which must merge the data from the two tapes, but the effective time resolution is about twice that of the normal mode.

Test Mode. The test mode is intended as an aid to the operator in assuring that the system is operating and adjusted properly, and is periodically recording calibration data on tape, for later use in reducing the data. It should allow the operator to detect serious interference or serious malfunction of the system, and to perform any necessary adjustments.

The calibrate function should be a complete calibration of the system, performed under operator supervision, and is in addition to any routine calibration function that may be automatically performed when the system is operating in one of the other modes. Known test signals are injected into the radiometer, and the resulting output digitized and recorded on tape just as in normal operation. Then the data are read from the tape and analyzed, with the results presented to the operator via the teletype and the monitor scope. The test data would then normally be left, appropriately labeled, at the head of the tape when normal operation is begun, to be available when the data are reduced.

3.5.3 Magnetic Tape Formats. All magnetic tapes are written in the standard 7-track format, with a density

of 556 characters per inch, with record lengths no greater than about 1000 words. All binary records are organized into 12-bit words (2 characters). Tapes are organized into files, where a new file begins at the start of every tape, and every time there is a change of mode or an interruption in the sampling routine. Each file consists of a label record, followed by a number of data records and calibration records.

Label Record. The label record is a BCD record containing the necessary information to identify and interpret the data which follow. It should contain:

1. The date and time of the start of the file.
2. The tape number and file number.
3. The radiometer channel assignments.
4. The sampling sequence.
5. The integration time for the radiometers.
6. The gain settings for the radiometers.
7. The mode of operation of the radiometers: Switching polarization, calibration sequence, etc.
8. The data format for the file.
9. The operator's identity.
10. Comments entered by the operator pertaining to weather, condition of the equipment, indications of interference, etc.

Since these items are all in BCD format, they may be conveniently extracted to identify printout or plots that may be generated in the course of processing the data.

Normal Data Record. A normal data record is a binary record, consisting of about 40 words of housekeeping and reference data, followed by 1000 samples from the radiometer, with little or no processing. Sufficient housekeeping data is included at the head of each record so that each record can almost stand alone during later processing, with little need for the processing programs to carry reference data from one record to another. The housekeeping items should include:

1. A flag to identify a normal data record.
2. The date and time of the first sample in the record.
3. The tape, file, and record numbers.
4. The radiometer channel assignments.
5. The channel sampling sequence.
6. The radiometer integration time.
7. The radiometer gain settings.
8. The mode of operation of the system.

There is much redundancy between the housekeeping data in the data record and the label record. This redundancy is not particularly wasteful,

since only small amounts of information are involved, and should contribute to the efficiency of the processing programs.

Condensed Data Records. The condensed data records use essentially the same format as the normal data records. The first-word flag identifies a condensed data record. The radiometer sampling sequence, integration time, and channel assignments are replaced by the appropriate synthetic values. If, for example, the condensed record were formed by averaging several samples which were consecutive in time, the effective integration time is increased, and the sampling rate reduced. If it were formed by averaging together two or more channels which are adjacent in frequency, then the synthetic channel assignments are given. If these housekeeping items are properly interpreted, it will be possible in many instances to process both normal and condensed records using the same programs.

Calibration Records. A calibration record is inserted whenever a major calibration of the system is performed. Such a calibration would normally be performed every morning before operations begin, and perhaps at other times as well. A

calibration record is a binary record whose format is not yet specified, except that it must begin with a flag which identifies it as a calibration record. The format can probably be made to closely resemble a normal data record, except of course, that it must contain enough information to specify the values and sequence of the calibration signals.

Special Formats. Special modes of operation will no doubt require special data formats. Any format may be employed, provided that the first word is a flag to identify the format.

3.5.4 Programming. A separate program package will be required for each mode of operation of the system, though the different modes will share many subroutines. Each package will consist of a main program, which determines the basic sequence of operations in that mode, and a set of subroutines which carry out these operations. Changing the operating mode of the system will, then, require that a different program package be read into the controller, though in some instances the programs may be sufficiently similar that one package can support two modes of operation.

Program Package for Normal Mode. The principal components of the program package for the normal mode are listed here. The components for the other modes will be quite similar.

1. Main Program: Calls subroutines in proper order, and monitors their execution. Responds to interrupts from I/O devices, direct access channels, and from operator's console.

2. I/O Control Packages: Packages to control the console teletype, magnetic tape units, and MX/ADC. Handle the details of input and output when called by main program.

3. Data Condenser: Averages high-resolution data to produce condensed data, according to parameters transmitted by the main program.

4. Solar Activity Test: An algorithm for testing the incoming data to determine whether solar activity appears to be present or not. Returns a "yes" or "no" to the main program, which takes appropriate action to save or destroy the high-resolution data.

5. Housekeeping Data Generator: Samples the various housekeeping and reference data items, formats, scales them, and stores them in the proper output arrays, ready to be inserted into the label records and data records.

6. Operator Monitor: Generates printout which serves as a log of the system operations, and as a source of monitoring information to the operator. Also accepts and interprets directives from the operator. Operator directives may change the mode

of operation of the system, change the value of some parameter, such as the sampling rate, or insert data into the label records, such as comments about the observing conditions, etc. Also generates appropriate plots on the monitor scope to allow the operator to inspect the data.

Supporting Software. It is anticipated that, as we learn more about the behavior of the sun as seen at centimeter wavelengths with high time resolution, we will wish to modify the observing procedures, data formats, and data processing procedures. All of these activities will require modifying programs and writing new ones, sometimes on very short notice. Thus, wherever possible, the programs should be written in a higher level language, and in direct and straight-forward fashion. Supporting software for the system should include:

1. A symbolic assembler.
2. A compiler for FORTRAN or similar language.
3. A magnetic tape operating system, capable of generating self-loading binary program tapes for the various program packages.
4. A text editor for source programs.

Data Reduction and Analysis. We anticipate that most of the reduction and analysis of the data will be performed on the existing UM/RAO XDS 930 computer

located in the Space Research Building, on the University of Michigan's North Campus. It will be highly desirable, however, to also perform at least some of the data testing on the data acquisition system at the Radio Telescope Site. This capability would be useful to occasionally present a portion of the data for immediate inspection.

Solar Activity Test Algorithm. At the maximum data rate for the normal mode, the system fills more than five magnetic tapes per hour, or about 50 tapes per day. It is anticipated that solar activity that requires millisecond time resolution will be infrequent. Hence a considerable saving in tape consumption and processing time will result if high-resolution data are preserved only for those periods when solar activity appears to be present. We propose to include a simple algorithm in the control program which tests whether or not high-resolution data should be preserved.

The form of the algorithm is not yet specified, and no final form can be specified until there is a reasonable amount of high-resolution data available for study, and something is known about the fine structure of solar activity in the spectral

region from 2 to 8 GHz. The general approach, then, will be to include a crude algorithm in the program, and to apply it to all data gathered, recording the result, but saving a reasonable quantity of high resolution data regardless of the algorithm. Analysis of this data will allow us to evaluate the algorithm, and hopefully to improve it, until we have sufficient faith to use it.

Two forms of the algorithm may be postulated for testing; a simple amplitude discrimination scheme, and a more sophisticated spectral analysis.

The amplitude discrimination scheme monitors the average brightness temperature, as measured by the radiometer. When this temperature deviates outside of a preset range, activity is assumed to be present.

The spectral analysis scheme is more generalized, but more costly. A simple spectral analysis is performed on the data samples to detect the presence of fluctuations whose characteristic period lies in the range where it would be resolved by the high resolution data, but not in the condensed data. This range includes periods between a few milliseconds and a few tenths of a second. The

spectral analysis scheme makes no assumptions about the nature of solar activity. It simply preserves high-resolution data when, and only when, there are components present in the signal that would otherwise be lost. Thus it will not discriminate between solar activity and pulsed interference.

3.6 SYSTEM EXPANSION AND CONTRACTION

One of the secondary goals of this design effort was to develop a system which was easily expanded or contracted. We feel that we have been far more successful in achieving expansion capability than in the ability to reduce or contract the system. The primary reason for this is that the proposed system is very close to an optimized balance of science and cost as will be shown below.

3.6.1 Recommendations for Expansion.

The top priority item in system expansion is the addition of frequency coverage from 12 to 18 GHz.* In this frequency range, the quiet sun temperature is approximately 10^4 °K, and if we assume the same value for the maximum flux density from a solar burst as that in the X band region of approximately

* See note at end of Section 3.6.2

3×10^4 fu, the maximum antenna temperature expected would be on the order of 1.2×10^6 °K. This assumes that the antenna beam is smaller than the solar disc. The dynamic range would be 21 dB, and again some form of compression of the signal is required.

Rapid switching for time duplexing of the polarization is no longer feasible in this frequency range. Ferrite switches that cover the 12-18 GHz are available, but the switching speed is on the order of 15 milliseconds. Higher speed switches (switching times less than 100 μsec) have bandwidths on the order of 1 GHz. Therefore, to receive both polarizations, it appears that either time resolution must be sacrificed or a separate receiving channel for each polarization is required.

To extend the frequency range, another antenna system is required. Reflectors are available with diameters up to 150 feet with sufficient surface accuracy to use in this frequency range. A parabolic reflector 18 feet in diameter with a surface accuracy of 0.015" (0.023 mm) is available and suitable for this application. With this surface accuracy, the reflector would be useable

well into the mm-wavelength region. The beamwidth of the antenna can be calculated from the expression

$$W = 227'/f$$

Thus the beamwidth at 8 GHz is 28'; at 12 GHz, 19'; and at 18 GHz, 12.5'. At 4 mm (75 GHz) the beamwidth would be 3' . SCR-584 pedestals are available for mounting the antenna. These pedestals were part of an S-band fire control system and supported a 6-foot parabola. These pedestals have been used with dishes as large as 20-foot in diameter. The static accuracy of the pedestal is approximately 0.5 milliradian (1.7') which is adequate for this application. Further evaluation of the pedestal is required to determine if it would be useable for higher frequency work. A six-channel receiver similar to that used in the S and C bands would probably be the best approach. TWT's would be used as preamplifiers followed by filters and feedback detector systems. Two channels would be used, one for each sense of polarization. Figure 4 is a block diagram of the basic receiver.

The receiver specifications are listed below.

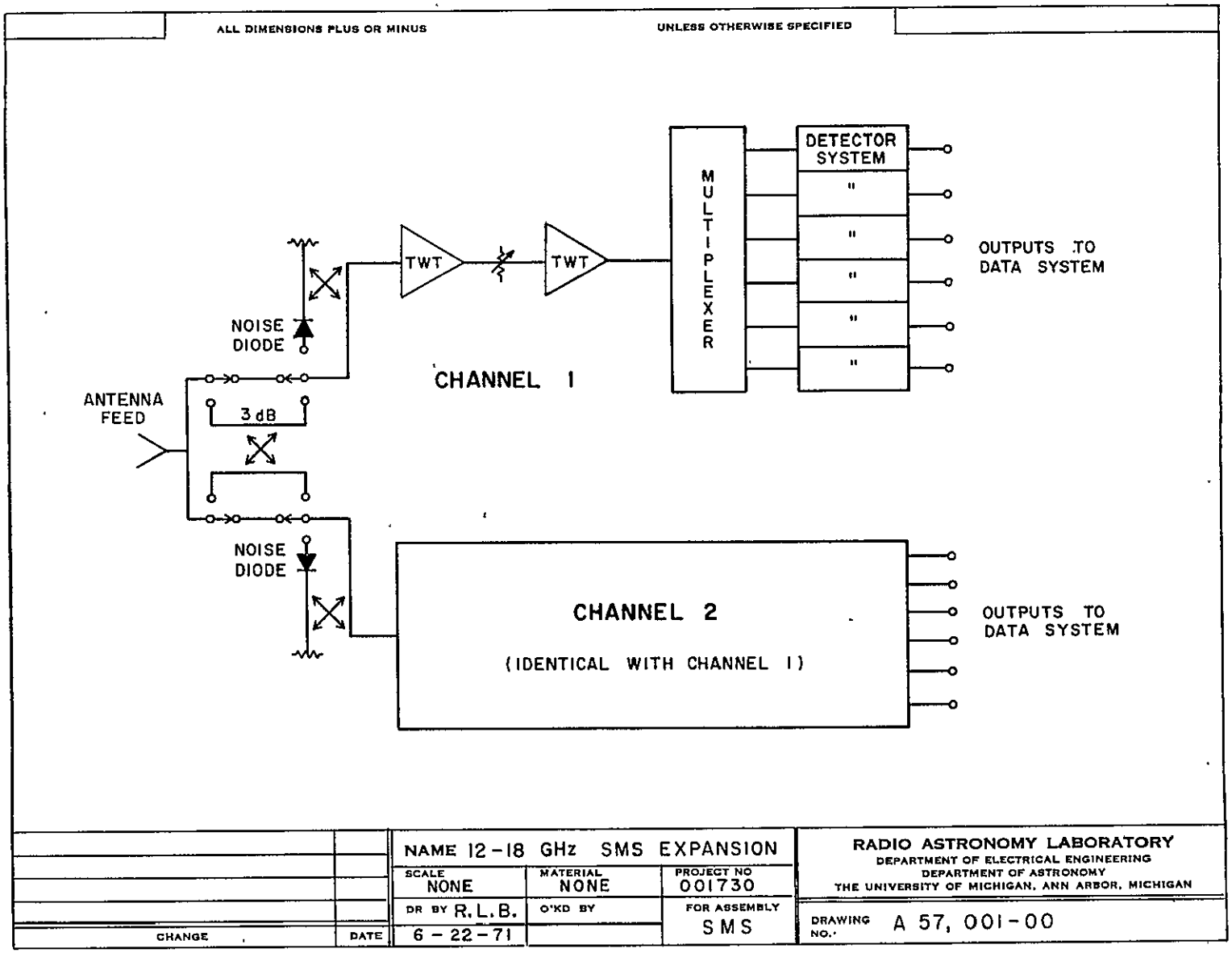

Figure 4. Proposed 12-18 GHz SMS Expansion Block Diagram

Frequency Range	12-18 GHz*
Noise Figure	10 dB
Channel Bandwidth	1 GHz nominal
Channel Spacing	1.2 GHz nominal
Receiver Fluctuation Noise ($\tau = 10^{-4}$s)	<0.3% of the received signal
Antenna Beamwidth	19' to 12.5'

3.6.2 Recommendations for Contraction. If we define contraction as the reduction in cost without compromising the scientific goals, we find that very little contraction is possible. The proposed system design goals included reasonable cost but in fact came closer to minimum cost. If we examine the operational modes of the system, the block diagrams, and the equipment lists, we find that the only item which can be deleted without significantly compromising the scientific goals is one magnetic tape recorder. The normal mode of operation requires three tape recorders and these tape recorders must be shut down periodically to have preventative maintenance performed on them. During this down time, the system cannot be operated in the normal mode. The penalty of lost observation time is quite high when compared to the cost

---

*See note at end of section 3.6.2

of the tape recorder.

A further use of the fourth tape recorder is to change operational modes efficiently with minimum loss of observational time.

*NOTE

A TWT that will cover the entire 8-18 GHz range is available from Watkins-Johnson. However, this was not discovered in time to study the possibility of extending the antenna feed and radiometer to cover the 8-12 GHz frequency range.

4. COST TO IMPLEMENT SYSTEM

The anticipated cost of the SMS system proposed above is based on the present prices of the catalog items, vendor bids for non-catalog items, estimated costs for in-house constructed items, and estimated FY 1972 manpower and burden rates. This cost is presented in section 4.1. Scientific guidance is provided at no cost.

The anticipated cost of the MINIMUM SYSTEM is contained in section 4.2 and is based on the recommendations presented in section 3.6.1. This anticipated cost is very close to the cost estimate for the proposed system.

The anticipated cost of the EXPANDED SYSTEM is contained in section 4.3 and is based on the recommendations presented in section 3.6.2. This anticipated cost estimate is not as accurate as the cost estimate for the proposed system since time did not permit as accurate an analysis.

4.1 PROPOSED SYSTEM

The proposed system has been designed to achieve the scientific goals with little in the way of superfluous equipment. It is a good compromise between initial installation cost and operational expense and has the capability of being easily expanded in the future.

4.1.1 Antenna and Feed. The necessary repair, maintenance, and site preparation work (which was outlined in section 3.3) required to use the 28-foot antenna and equipment house for this system has been estimated at $3500 for parts and outside labor, and 3 man-months of site personnel effort. The initial bids and estimates for the antenna feed range from $3000 to $4000. The additional effort necessary to mount this feed on the antenna is estimated at one man-month. The estimated cost for the antenna and feed system is shown below.

4.1.2 Receivers. In addition to the cost of the receiver, an additional head is required for the Alfred sweep generator to cover the 2-4 GHz portion of the spectrum. The head is Model 652-S5 and covers the frequency range of 1.7-4.2 GHz. The price of $2,050 with a delivery time of 3 weeks. The detailed breakdown of the receiver costs is contained in Appendix F, followed by a description of the individual items. No spares are included in the estimates.

A considerable amount of manpower will be required to obtain an operating receiver. The tasks involved are as described in section 6.1.2. The estimated cost for the receiver is presented below.

4.1.3 Data Processing and Storage. The estimated cost of the data processing and storage portion of the system is presented below. In addition to the equipment contained in Appendix G, considerable manpower will be required to perform the equipment programming tasks described in sections 6.1.3 and 6.2. The equipment cost contained in Appendix G is representative of the maximum equipment cost (acceptable equipment by a competing manufacturer may be available at a lower price) for the data acquisition equipment as the cost is based on actual catalog prices of an acceptable subsystem.

EXCLUDED COSTS (1) No data tape costs are included in this cost estimate. These tapes should be GFE because NASA/GSFC can procure these tapes at a far lower cost than can be obtained by independent purchasers. (2) No master timer equipment costs have been included since the absolute time accuracy required is not presently known.

4.1.4 Total Cost Estimate. The total cost estimate is the sum of the individual sub-systems, estimated in sections 4.2.1 through 4.2.3. This cost is shown below. Scientific guidance is provided at no cost.

28 FOOT ANTENNA AND FEED COST ESTIMATE

MANPOWER

	Time (M.M.)	FY'72 Wages
Engineer	2	$ 2,915
Technician	1 1/2	1,169
Technician	1 1/2	1,405
	Salaries	$ 5,489
Fringe Benefits @ 12% Est.		$ 659
Total Wages and Fringe Benefits		$ 6,148
Indirect Cost @ 54.4% (Predetermined for FY'71, Est. FY'72)		$ 3,345
Total Manpower Cost		$ 9,492

EQUIPMENT

Misc. Supplies and Communications	$ 125
28-ft. Antenna Refurbishing	3,500
Feed	4,000
Equip. Subtotal	$ 7,625

TOTAL COST $17,117

RECEIVER COST ESTIMATE

MANPOWER

	Time (M.M.)	FY'72 Wages
Engineer	6	$ 12,720
Engineer	19	27,693
Technician	9 1/2	7,402
Technician	9 1/2	8,896
Clerical & Drafting	6	3,180
Administration	3	5,112
	Salaries	$ 65,003
Fringe Benefits @ 12% Est.		$ 7,800
Total Salaries and Fringe Benefits		$ 72,803
Indirect Cost @ 54.4% (Predetermined for FY'71, Est. FY'72)		$ 39,605
Total Manpower Cost		$112,408

EQUIPMENT

Misc. Supplies and Communications	$ 2,162
Alfred Sweep Generator Head	2,050
Basic Receiver Parts (No Spares)	40,426
Spare Parts - Est. @ 10%	3,483
Equip. Subtotal	$ 48,121

TOTAL COST $160,529

DATA PROCESSING AND STORAGE COST ESTIMATE

MANPOWER

	Time (M.M.)	FY'72 Wages
Engineer	7	$ 7,420
Technician	2	1,873
Technician	2	1,420
Analyst	6	11,130
Programmer	7 1/2	7,444
Clerical & Drafting	6	3,180
Administration	2	3,408
	Salaries	$ 35,875
Fringe Benefits @ 12% Est.		$ 4,350
Total Salaries and Fringe Benefits		$ 40,225
Indirect Cost @ 54.4% (Predetermined for FY'71, Est. FY'72)		$ 21,882
Total Manpower Cost		$ 62,107

EQUIPMENT

Misc. Supplies and Communication	$ 1,688
Basic Data Processing and Storage Parts (No Spares)	65,720
Spare Parts - Est. @ 10%	6,572
Equip. Subtotal	$ 73,980

TOTAL COST $136,087*

*See excluded costs, Section 4.1.3

TOTAL PROPOSED SYSTEM COST

Antenna and Feed Total	$ 17,117
Receiver Total	$160,529
Data Processing and Storage Total	$136,087
TOTAL MODERATE SYSTEM COST	$313,733

4.2 MINIMUM SYSTEM

The equipment that is required to implement the minimum system is essentially the same as for the proposed system. The reasons for this were explained in section 3.6.2 above. The cost of the minimum system is therefore essentially the same as for the proposed system if all of the equipment is purchased.

One possible way to reduce costs is to obtain government furnished equipment (GFE) instead of purchasing new equipment. (The entire cost of the purchased equipment replaced by GFE is not saved because additional manpower is usually required to refurbish the equipment.) The likelihood of finding GFE for the radiometer or antenna equipment is probably very slim. The data acquisition and recording equipment holds far more promise of being obtainable as GFE. This is due to the normal equipment updating cycle and the fair number of small computers within the government laboratories. This is particularly true of the tape recording equipment which is slow compared to present standards and has seven tracks instead of the new nine track format. The master timing unit is another area where GFE may be available since many of the old 10^{-9} clocks are being replaced by much higher accuracy units.

4.3 EXPANDED SYSTEM

The cost to implement the expanded system is presented below as the cost of the expansion plus the cost of the proposed system. The cost estimates for the expansion are not as accurate as for the proposed system. Scientific guidance is provided at no cost.

The estimated cost of the equipment for the expansion is:

Antenna & Feed	
Reflector	$12,500
Pedestal	1,000
Feed	2,000
3-dB hybrid	100
Waveguide switches (2)	1,000
Subtotal	$16,600
Receiver	
4 TWT	$22,000
2 Directional couplers	400
2 Multiplexers	3,000
12 Detector/Filter systems	12,000
2 Attenuators	300
Miscellaneous electronics, power supplies & packaging	3,000
16-Channel multiplexer & A/D converter	2,100
Subtotal	$42,800
Total equipment for expansion --	$59,400.

TOTAL EXPANDED SYSTEM COST

MANPOWER

	Time (M.M.)	FY'72 Wages
Engineer	12	$ 17,490
Technician	12	11,236
Programmer	2	1,985
Clerical & Drafting	6	3,180
Administration	2	3,408
	Salaries	$ 37,299
Fringe Benefits @ 12% Est.		$ 4,476
Total Salaries and Fringe Benefits		$ 41,775
Indirect Cost @ 54.4% (Predetermined for FY'71, Est. FY'72)		$ 22,726
Total Manpower Cost		$ 64,501

EQUIPMENT

Misc. Supplies and Communications	$ 1,118
Expansion Parts	59,400
Spare Parts - Est. @ 10%	5,730
Equip. Subtotal	$ 66,248

TOTAL EXPANSION COST	$130,749
PROPOSED SYSTEM COST	$313,733
TOTAL EXPANDED SYSTEM COST	$444,482

5. OPERATION COSTS

The production of useful scientific data from the SMS will require considerable effort. Since this is an instrument which is capable of acquiring data which has been unavailable heretofore, the SMS operational modes, data reduction programs, and data presentation formats cannot be predicted with certainty. It is for this reason that the operation of the instrument must be treated as a dynamic interaction of scientists, programmers and engineers and not as a production facility.

The programming effort, and the necessary scientific guidance, should be started six months prior to the completion of the construction and testing of the SMS. This is necessary if operations are to begin immediately since this effort has not been included in the cost estimate for the instrumentation phase.

The effort required to produce useful scientific data from the operational SMS for the first and second year is presented below and is based on the following assumptions:

(a) The SMS will be in operation whenever the sun is in a favorable position.

(b) The SMS operator will also be the technician responsible for maintaining the equipment.

(c) All magnetic tape will be obtained as GFE, Government Furnished Equipment at no cost to the project.

(d) The data reduction will be performed at the UM/RAO data processing facility. This facility was provided by the OGO Program at GSFC.

(e) The engineering support required for the maintenance of the SMS will be provided by presently available personnel.

5.1 DATA ACQUISITION TASKS

The tasks that must be performed to acquire the data are as follows:

1. Train and Supervise Operators. The task of training and supervising the system operators is normally perfomed by a programmer. This is a continuing task, but does not require much time.

2. Operation of the Data Acquisition Equipment. An operator must be on call whenever data is being recorded to monitor the operation of the system, change magnetic tapes, etc. These tasks should keep him busy only about 1/4 of the time.

3. Write the Data Acquisition Programs. Programs must be written for the data acquisition system to input data from the analog-to-digital converter, format it for magnetic tape, and output it to tape, along with controlling the entire operation. A different program package is required for each different mode of operation of the system. These "production' programs may be partially based upon the preliminary programs written during the instrument development phase

but will probably support additional modes of operation and possibly more complex operations.

A data acquisition program package will consist of a main program which calls a set of subroutines, most of which will be library subroutines, shared with other main programs. The main program will determine the mode of operation, the sampling sequence for the radiometer channels, and the format of the data. Subroutines, probably written in machine language, will be required to control the multiplexer, analog-to-digital converter, and the magnetic tape units, perform any checks to determine if the data samples have "reasonable" values, do any averaging or other statistical operations that may be required, perform any scaling or change of units, and perform any tests for probable solar activity.

4. Develop an Algorithm for Recognizing Probable Solar Activity. The cost of reducing the data gathered by this instrument is almost directly proportional to the quantity of data reduced. The cost of data reduction can be minimized by pre-filtering the data to preserve only those intervals of time which appear to include activity. The algorithm which performs this pre-filtering is therefore an important factor in

determining the cost of the data reduction. A good algorithm can be developed only after some data are inspected, and can be tested only by applying it to a sizeable sample of data which is also plotted and visually inspected for evidence of activity.

5. Participate in Staff Project Evaluation and Generation of New Operational-Modes and Procedures. This task is self explanatory.

6. Write Programs to Support New Modes of Operation. During the operation of the SMS instrument, knowledge will be gained that will suggest modifications to the observing procedures to obtain a more useful output. The SMS observing procedures are embodied, to a great extent, in the programs for the data acquisition system. Hence a new program package must be generated to implement a new mode of observation. The program package and the software system for the data acquisition system should be set up so as to facilitate the generation of new program packages. However, some effort will be required whenever a change is made. It is important to maintain sufficient flexibility that the system may be modified as needed, as new information comes to light.

7. Maintain Software for the Data Acquisition System. One of the objectives of the experiment is to maintain sufficient flexibility in the instrumentation that the

operating modes may be changed in response to the increasing knowledge of the nature of the rapid solar activity in the frequency range from 2 to 8 GHz. Every change in operating mode requires a change in the program package for the data acquisition system. These changes can be made quite easily and quickly if a good systems software package is made available. For some of the different controllers which are candidates for inclusion in the system, extensive operating systems have been written by various users, and may be available for adaptation. The ideal arrangement would be one in which a scientist with a minimum knowledge of systems programming could implement new observing modes, or modify existing modes. Generating and maintaining a software system that will allow this requires an experienced systems programmer.

8. Write Data Acquisition Portion of Contract Reports. This task is self explanatory.

5.2 DATA REDUCTION TASKS

The following tasks must be performed to reduce the data acquired by the SMS:

1. Train and Supervise Operators. The task of training and supervising the system operators is normally performed by a programmer. This is a continuing task, but does not require much time.

2. Operation of the Data Reduction Facility. The initial steps of reducing the data will be performed on a routine basis at the Data Processing Facility of the Radio Astronomy Observatory. A computer operator must be in attendance whenever the system is operating. It is expected that this task will be performed by the same operators who perform the data processing for the space experiments. The principal output of the initial data processing will be data plots on 35-mm film. The films will be developed by the operator, using the automatic film processor which is available at the data processing facility.

3. Maintain Files of Data Tapes and Films. The experiment will generate large numbers of magnetic tapes and 35-mm films containing experiment data. These must be properly labeled and filed in a systematic manner, so that specific data may later be retrieved, as required.

4. Write the Data Reduction Programs. Programs must be written to perform the routine data reduction operations. These programs will be written in FORTRAN with machine language subroutines, to run on the XDS 930 computer in the UM/RAO Data Processing Facility. These programs must be capable of accepting data in the form of the magnetic tapes generated by the data acquisition system, and must perform initial reduction of the data, generating graphic output on 35-mm film and hi-resolution plots, ready for examination and evaluation.

Magnetic tape handling routines are already available for the 930 which will perform most of the functions required for this application. Functions which must be added include provision to transform data samples written in the 12-bit words of the data acquisition system into the 24-bit internal format of the 930, and provision to search the data tapes for samples taken at a particular time. The capability of properly responding to such conditions as end-of-file, end-of-tape, and read check error is required, and is present in the available software in a form that is probably adequate.

The data reduction operations to be performed at this point include correction for instrument characteristics, optional averaging in both time and frequency, and perhaps some simple test for reasonableness, to discard or flag samples which are obviously erroneous. Particular care must be taken in programming the correction for instrument characteristic, since this operation could become very time consuming. It is necessary to correct each sample for the gain characteristic of the particular radiometer channel. The radiometer is approximately logarithmic, and it is probable that at this point we will wish to make an empirical correction to convert the pseudo-logarithmic radiometer output into a number which is proportional to the logarithm of antenna temperature. This conversion can be per-

formed by a machine-language subroutine, using integer arithmetic, and hence can be quite rapid.

Graphic output for initial inspection and evaluation can be computer-generated plots, either on paper or on 35-mm film. The UM/RAO Data Processing Facility currently has available both hardware and software capability to generate both forms of output. Perhaps some modifications or augmentations to the system will be required to increase the efficiency for this particular kind of data. A particular problem arises from the vast quantity of data which will be generated if the proposed system is operated at a sampling rate near its maximum for any appreciable fraction of the available operating time.

5. Participate in Staff Project Evaluation and Generation of New Operation Modes and Procedures. This task is self explanatory.

6. Write Programs to Support New Modes of Operation. This task consists of modifying the data reduction programs generated in task 4 above to accommodate new data acquisition data formats. If existing programs cannot accommodate the new formats, new programs will have to be written.

7. Write Programs for Detailed Analysis. Because of the vast quantity of information gathered by the proposed instrument for even short periods of solar activity, computer processing seems to be required for almost any detailed analysis. It is impossible to define procedures

for detailed analysis before some data are in hand, but statistical procedures are almost certain to be required. Processes which might be involved include Fourier transforms and autocorrelation to analyze the time behavior of the flux, correlations of the microwave flux with X-ray flux, optical radiation, low-frequency radio flux, proton flux, and other observable quantities which are associated with solar activity. Burst profiles will be analyzed to determine the rise and decay times, and periodicity in the bursts will be sought. All of these operations require the use of a computer if large quantities of data are to be processed. Some may require an interactive capability, where a scientist can view intermediate results, and guide the course of the computer program. Most of them can be performed more efficiently if a professional programmer works very closely with the scientist, so that procedures may easily be tried and modified.

8. Prepare Data for Presentation. Some programming effort will be required to process data for the generation of plots or tables suitable for publication, comparison with results of related experiments, and distribution to interested scientists.

9. Maintain Software for the 930 Computer. The software system presently in use for the XDS 930 computer in the UM/RAO Data Processing Facility has been

especially developed for reducing radio astronomy data from both space and ground-based observations. The services of an experienced systems programmer are required to maintain this system, to train operators in its use, and counsel scientists in its capabilities. Some augmentation and modification of the system will probably be advantageous to the solar observing program. The cost of maintaining this software will be shared among the various projects using the facility on a pro-rated basis.

10. Supervise Data Processing Operations. This task includes a pro-rated share of the supervision of the UM/RAO Data Processing Facility, and the supervision of the programming and hardware work on the data acquisition subsystem.

11. Write Data Processing Portions of Contract Reports. Data processing represents a large share of the work during the operational phase of the project. It must be reported upon since it has a bearing in the interpretation of the reduced data.

5.3 DATA ANALYSIS TASKS

A meaningful analysis of the data will require a completion of the following tasks.

1. Data Analysis. A radio astronomer must analyze the data to obtain the scientific results.

2. Propose New Operational Modes and Procedures. Propose new data acquisition modes and operational procedures based upon data analyzed and on scientific theory. This task also includes participation in staff project evaluation and planning.

3. Prepare Data for Presentation. Some processing of the data will be required to generate plots or tables suitable for publication, comparison with results of related experiments, and distribution to interested scientists.

4. Report on Scientific Results. The scientist will report on the scientific results of the data analysis by publishing papers and preparing the final scientific report.

5.4 INSTRUMENTATION TASKS

The instrumentation tasks are primarily directed toward the maintenance of the SMS instrument but also include the engineering and technician tasks necessary to improve the equipment performance.

1. Maintain Data Acquisition Equipment. Maintenance of the data acquisition equipment includes care and updating of the equipment maintenance documents and diagnostic programs, periodic checkout and preventive maintenance, and repair of breakdowns. Periodic cleaning and adjustment of the magnetic tape units will probably account for a major share of the effort.

2. Maintain Data Reduction Equipment. Both routine and emergency maintenance are included, pro-rated among the various projects which use the equipment.

3. Maintain the Antenna and Radiometer. Maintenance of the antenna and radiometer includes care and updating of the equipment maintenance documents, periodic checkout and maintenance, and repair of breakdowns.

4. Participate in Staff Project Evaluation and Generation of New Operational Modes and Procedures. This task is self explanatory.

5. Make Hardware Modifications to Support New Modes of Operation. This task is intended to cover only small modifications in operating mode which may be implemented more economically by modifying the data hardware, rather than the software. Major upgrading of the equipment is assumed to be separately funded.

SMS OPERATIONAL COST ESTIMATE
(First Year Operation)

MANPOWER

	Time (M.M.)	FY'72 Wages
Scientist	12	$ 15,900
Engineer	8 1/2	10,203
Technician	18 1/2	15,852
Analyst	11	20,405
Programmer	15	14,888
Operator	15 1/2	8,544
Clerical & Drafting	6	3,180
Administration	2	3,408
	Salaries	$ 92,380
Fringe Benefits @ 12% Est.		$ 11,086
Total Salaries & Fringe Benefits		$103,466
Indirect Cost @ 54.4% (Predetermined for FY'71, Est. FY'72)		$ 56,286
Total Manpower Cost		$159,752

EQUIPMENT

Misc. Supplies & Communication	$ 1,742
Computer Spare Parts	2,000
Film, Chemicals & Computer Paper	2,800
Equip. Subtotal	$ 6,542

TOTAL COST $166,294

SMS OPERATIONAL COST ESTIMATE
(Second Year Operation)

MANPOWER

	Time (M.M.)	FY'72 Wages
Scientist	12	$ 15,900
Engineer	7 1/2	9,002
Technician	16 1/2	14,140
Analyst	5 1/2	10,200
Programmer	5 1/2	8,188
Operator	15 1/2	8,545
Clerical & Drafing	4	2,120
Administration	2	3,408
	Salaries	$ 71,503
Fringe Benefits @ 12% Est.		8,580
Total Salaries & Fringe Benefits		$ 80,083
Indirect Cost @ 54.4% (Predetermined for FY'71, Est. FY'72)		$ 43,565
Total Manpower Cost		$123,648

EQUIPMENT

Misc. Supplies & Communication	$ 1,773
Computer Spare Parts	2,000
Film, Chemicals & Computer Paper	2,800
Equip. Subtotal	$ 6,573

TOTAL COST $130,022

6. IMPLEMENTATION PLAN

The objectives of the implementation plan are to complete the installation and checkout of the proposed system in the projected time period, maintain as continuous a manpower workload as possible, and schedule the delivery of equipment as needed such that the expenditure of funds is as level as possible. These objectives are compatible with minimizing costs and utilize the available UM/RAO personnel to best advantage.

6.1 INSTRUMENT CONSTRUCTION

There are three basic parts to the systems which must be scheduled to be completed in 18 months. The schedule for the antenna and feed has the least effect on the schedules for the radiometer or the data processing and storage subsystem. The schedules for the radiometer and data processing and storage subsystem are relatively independent with the exception that the analog data output terminals of the radiometer must be specified before the radiometer-to-multiplexer interface can be designed for the data subsystem. A PERT chart was not developed for this implementation plan due to the relative independence of the three basic parts.

6.1.1 Antenna and Feed. The schedule for the antenna and feed portion of the system is contained in Figure 5. The tasks outlined there are defined as follows:

1A. Refurbish 28-ft antenna and house. This task consists of refurbishing the mechanical drive system of the antenna, replacing the wiring between the antenna and the house, removing the obsolete equipment from the house to make room for the SMS equipment, and miscellaneous tasks to ready the house for the new equipment.

2A. Design and construct the antenna feed. This task consists of selecting the optimum feed combination for the two octaves, designing the feed, and constructing it. There will be some interaction with the receiver package design.

3A. Install and test the antenna feed. This task consists of a mechanical fit and alignment check plus a performance test of the antenna and feed at several discrete frequencies. A more comprehensive test will be done during the final system test.

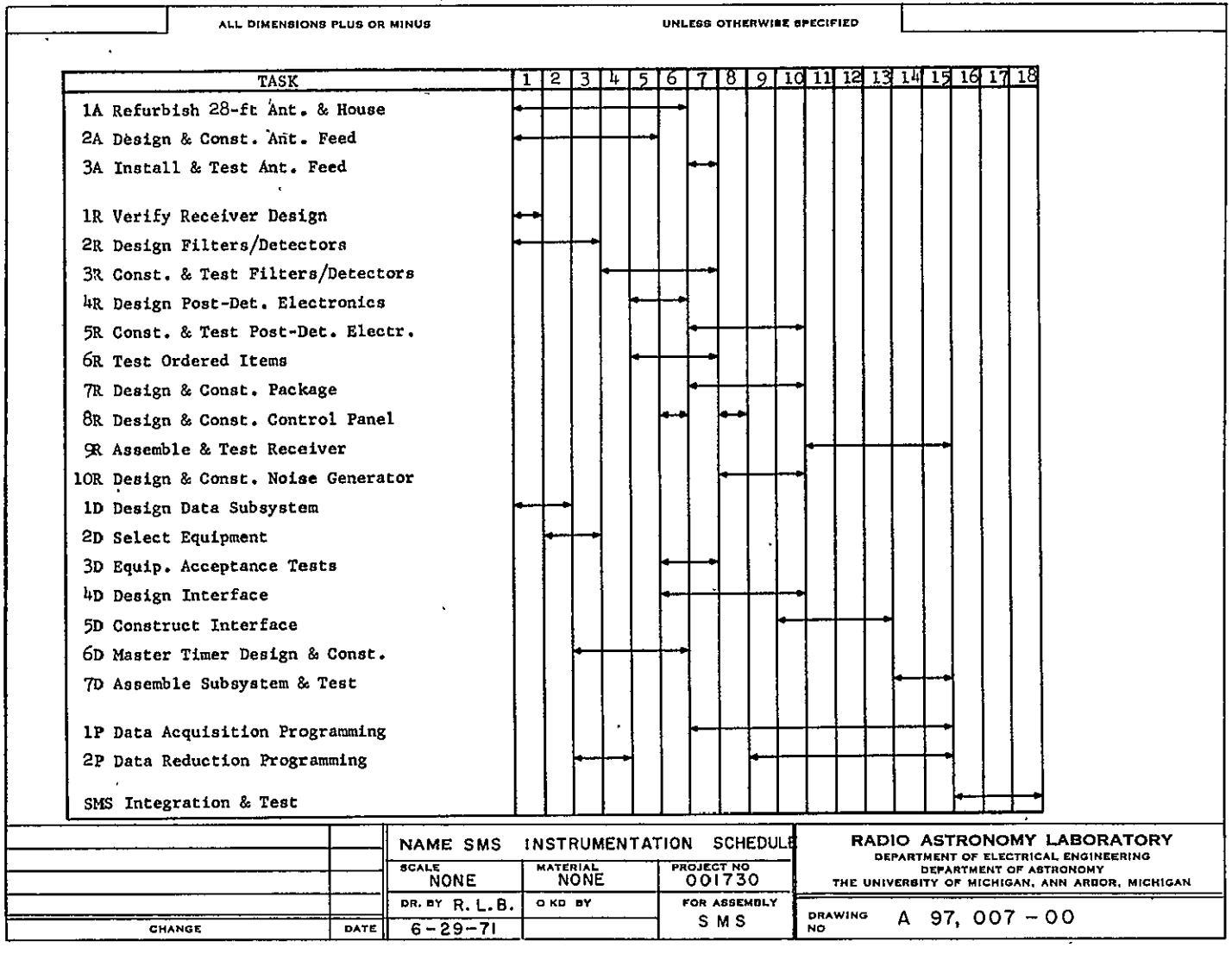

Figure 5. SMS Instrumentation Schedule

6.1.2 Radiometer. The schedule for the radiometer implementation is contained in Figure 5. The tasks outlined there are defined as follows:

1R. Verify receiver design. This task consists of reviewing this radiometer design, updating it if necessary, producing the list of items to be purchased, and generating the specifications for the in-house designed items.

2R. Design the filter/detector circuits. This task consists of designing and breadboarding the 10 channel per octave filters, matching networks, pin attenuators, and detectors for both the 2-4 GHZ and 4-8 GHZ portions of the radiometer.

3R. Construct and test the filter/detector circuits. This task consists of constructing the directional filter and the 10 associated channel-detectors for each of the two octaves.

4R. Design the post-detector electronics. This task consists of designing and breadboarding the post detector electronics for the 20 channel filters, and generating the interface specifications for the data processing and storage subsystem.

5R. Construct and test the post-detector electronics. This task consists of constructing the post-detector electronics for the 20 channels and testing them in conjunction with the appropriate filter/detectors.

6R. Test ordered items. This task is simply to perform the visual, electrical, and mechanical tests necessary to assure that the purchased items are as specified.

7R. Design and construct the package. This task consists of designing the radiometer housing to be compatible with both the 28-foot dish and the 85-foot dish, to contain all of the necessary equipment items, and to be easily serviced.

8R. Design and construct the control panel. This task consists of determining what indicators and contro should be placed on the control panel and then designing the panel and interface. This task must be a joint effort by all design engineers.

9R. Assemble and test the receiver. This task is self explanatory.

6.1.3 Data Processing and Storage Subsystem. The schedule for the data processing and storage subsystem is contained in Figure 5. The tasks outlined there are defined as follows:

1D. Design the data subsystem. This task consists of re-evaluating the proposed design in the light of the then available data systems to obtain the best subsystem at the least cost.

2D. Select equipment. This task consists of evaluating several competing data systems to determine which provides the best performance/cost and then ordering the equipment. A complete set of specifications for the ordered equipment must be obtained at this time in order to proceed with the interface design.

3D. Equipment acceptance test. This task consists of preparing and performing the acceptance tests for the data subsystem, including the instrument controller, its peripheral devices, and its software.

4D. Design the interface. This task consists of designing all of the necessary interfaces between the data subsystem and the remainder of the SMS. Provisions must be made for remotely locating the multiplexer and A/D converter, and for future expansion of the SMS.

5D. Construct the interface. This task is self explanatory.

6D. Master timer design and construction. This task consists of designing and constructing the time base generator and associated hardware which provides for accurate timing of the radiometer samples and correlates this timing with WWV.

7D. Assemble subsystem and test. This task consists of assembling all of the hardware which was not included in the equipment acceptance tests and the testing of the subsystem.

6.2 INSTRUMENT PROGRAMMING

The instrument programming tasks contained in the schedule shown in Figure 5 must be completed prior to the SMS systems tests. In fact, some of the programs must be completed prior to the data processing and storage subsystem test (task 7D). The data equipment acceptance tests (task 3D) can be completed by running the equipment diagnostic programs supplied by the manufacturer with very little programming supplied by the UM/RAO staff.

The availability and applicability of existing programs for the selected instrument controller, data formatter, and associated peripheral equipment is unknown at the present time. However; it is felt that some programs will be available either from the manufacturer or from the users group. It will be necessary to gather all of the available and applicable programs.

The programming tasks presented in Figure 5 are defined as follows:

1P. Data acquisition programming. This task consists of writing and debugging the initial versions of the programs for data acquisition and system mode control. The writing and execution of these programs will contribute to the programmers familiarization with the instrument.

These programs should stress flexibility rather than efficiency. They should be capable of sampling a specified set of radiometer channels at a specified rate, and provide the option of output via teletype, tape, or both. No solar activity detector algorithm is needed at this time and it is probably unimportant to include provision for accurate absolute time.

2P. Data reduction programming. This task consists of writing and debugging the XDS-930 programs necessary to reduce the data acquired by the SMS. These programs should be available during the check-out phase to perform such operations as analyzing the calibration data to determine the transfer function of the instrument, as well as listing and/or plotting the data from the tests.

7. KEY FACILITIES

The key facilities of the University of Michigan Radio Astronomy Observatory that will be necessary to implement the proposed solar measurement system are the radio telescopes and the data processing facility described below and in sections 3.3 and 3.5.

7.1 RADIO TELESCOPES

The facilities at the Radio Observatory include a 28-foot and a 85-foot parabolic antenna. The 28-foot antenna was constructed in 1956 and used for solar observations initially from 100-600 MHz, and later from 2-4 GHz. The receivers used were swept-frequency dynamic spectrum analyzers with a CRT-film recording system. The reflector is fiber glass with the reflecting material imbedded in the fiber glass. The antenna surface is accurate enough for use at wavelengths as short as 3 cm. There are also two buildings located at the 28-foot antenna site: an operations building housing the operating controls of the antenna and a smaller building at the base of the 28-foot antenna which can be used for equipment housing.

The 85-foot radio telescope was completed in 1959 and has been used for a variety of observing programs since that time. Radiometers operating at wavelengths of 37.5, 7.5, 3.75, 3.3, and 1.8 cm are presently available

and being used on this antenna. Rotating horn polarimeters and a spectral line receiver are also available for use with this radio telescope. The data recording system for this instrument uses a magnetic tape recorder to record data for later processing. Automatic control of the antenna is also available, and can provide automatic scans, on-off observations, and a number of other functions. The operations building houses the antenna controls, digital recording and control system, and the receiving systems. Laboratory space is also available for maintenance and development work.

In addition to the two operations buildings, another building at the Radio Observatory houses a small machine shop and additional laboratory facilities used for microwave development work.

7.2 DATA PROCESSING FACILITY

The data facility of the University of Michigan Radio Astronomy Observatory consists of an XDS-930 computer, and a special buffer-display system, designed and built by the staff. Software is based upon the XDS MONARCH system, supplemented by locally written subroutines for handling the special equipment.

The computer has a core memory capacity of eight thousand words, of twenty-four bits each, backed up by a disc of

250,000 words. It is provided with a real-time clock, sixteen priority interrupts, twenty-four special output lines (set lines), setable by program, and twenty-four special input lines (sense lines), whose state can be sensed by the program. The I/O devices on the computer are a teletype, card reader, high-speed line printer, and two seven-track magnetic units.

The special buffer-display system, designed and built by RAO personnel, includes a buffer core memory of four thousand words of thirty-six bits each, controlled by a stored-program I/O channel. I/O devices presently connected to the buffer-display include a direct-view CRT display, a photographic CRT display with an automatic 35mm camera, an incremental plotter, an input keyboard, and a magnetic tape unit. The I/O channel of the buffer-display system can transfer data between the buffer core and the computer, as well as between the buffer core and its own I/O devices, so the system can be used either in an on-line or off-line mode.

A "user's console", associated with the display unit, permits the user to communicate control decisions back to the computer. Thus the system provides for complete interaction between the user and the computer, via the display and user's console.

Special software, written by the UM/RAO staff, permits the entire system to be used by the FORTRAN programmer.

Library subroutines provide for graphic output on the direct view CRT, the photographic CRT, and the incremental plotter. Other subroutines permit the program to react to the pushbuttons, switches, and the "joystick" control on the user's console.

Two special off-line data facilities designed and built by the UM/RAO staff are the data logger and the tape-to-film converter. The data logger includes a fourteen-bit analog-to-digital converter and a sixteen channel multiplexer. Its function is to convert analog voltage signals to digital form, and record them on computer-compatible magnetic tape. The tape-to-film converter includes a small CRT display and a 35mm camera. Its function is to accept data on digital magnetic tape, and to generate intensity-modulated plots on film. Both of these units are in the process of being absorbed into the main data system.

APPENDIX A

SOLAR RECEIVER
SIGNAL-TO-NOISE RATIO ANALYSIS

The basic receiver used in this application is a DC radiometer. A wide-band preamplifier is used, followed by directional filters and detectors. While a feedback system at the detectors is planned, this analysis is based on a conventional configuration.

For a square law detector, the output voltage, E_{DC}, is

$$E_{DC} = \gamma P_{in} = \gamma [kBG(T_R+T_S+\Delta T_S)]$$

where γ is the detector constant (mv/mw)
k is Boltzman's constant (1.38×10^{-23} joules/deg)
B is the RF bandwidth preceding the detector (Hz)
T_R is the receiver noise temperature (K)
T_S is the quiet sun temperature (K)
ΔT_S is the increase in the sun's temperature due to solar activity (K).

The noise voltage at the detector output, N, is

$$N = \left[\frac{2B_V}{B} (P_{in})^2 + \left(\frac{N_D^2}{B_{eq}} B_V \right) \right]^{1/2}$$

where B_V is the video bandwidth of the detector output (Hz)
N_D is the noise voltage generated by the detector (v)
B_{eq} is the equivalent bandwidth of the detector noise voltage (Hz).

If we define the change in the output voltage due to changes in the solar temperature (ΔT_S) as the signal, then the signal-to-noise ratio (snr) is:

$$\frac{S^2}{N^2} = \frac{(\gamma kBG\Delta T_S)^2}{\frac{2B_v}{B}\left[\gamma kBG(T_R+T_S+\Delta T_S)\right]^2 + N_D^2 \frac{B_v}{B_{eq}}}$$

To evaluate the effect of the detector noise, we will use the Hewlett-Packard type 5082-2750 diode as an example. This diode is a Shottky-Barrier type which has the following characteristics[1]:

Tangential Signal Sensitivity (TSS)	-69 dBm
B_v	375 kHz
γ	5000 mv/mw
1/f noise corner frequency, f_c	2 kHz

The snr for a tangential signal is 8 dB; therefore, the detector noise corresponds to an input signal of -77 dBm and N_D is

$$N_D = \gamma P_{in} = 5000 \times 2 \times 10^{-8} = 10^{-4} \text{ mv or } 10^{-7} \text{ v} .$$

The spectral density, $G_D(f)$, is

$$G_D = \frac{N_D^2}{B_v} = \frac{10^{-14}}{375 \times 10^3} = 2.7 \times 10^{-20} \text{ v}^2/\text{Hz}.$$

where the low frequency cutoff of the video amplifier is greater than the noise corner frequency, f_c.

For video frequencies extending to less than f_c, the 1/f noise component must be included, and

$$G_D(f) = 2.7 \times 10^{-20} \left(1 + \frac{2000}{f}\right) v^2/Hz.$$

If the low frequency cutoff of the video amplifier is f_1, then the output noise voltage is

$$N_D^2 = \int_{f_1}^{B_v} G_D(f)df = 2.7 \times 10 \int_{f_1}^{B_v} \left(1 + \frac{2000}{f}\right)df$$

$$N_D^2 = 2.7 \times 10^{-20} \left[1 + \frac{2000}{B_v} \ln\left(\frac{B_v}{f_1}\right)\right]$$

For $f_1 << B_v$ such that $B_v - f_1 \approx B_v$. The equivalent spectral density, $G'_D(f)$, is

$$G'_D(f) = \frac{N_D^2}{B_v} = 2.7 \times 10^{-20} \left[1 + \frac{2000}{B_v} \ln\left(\frac{B_v}{f_1}\right)\right].$$

Using this expression for N_D^2/B_{eq} in the snr expression and simplifying,

$$\frac{S^2}{N^2} = \frac{B}{2B_v} \frac{(\Delta T_S)^2}{(T_R+T_S+\Delta T_S)^2} \cdot \frac{1}{1+ \dfrac{[1.35\times10^{-20}(1+\frac{2000}{B_v})\ln(\frac{B_v}{f_1})]B}{[\gamma kBG(T_R+T_S+\Delta T_S)]^2}}$$

To evaluate the term corresponding to the detector noise, we must consider this term separately for the two octaves of interest since T_S varies differently with frequency for the two octaves.

For the 2-4 GHz octave,

$$T_S = \frac{4 \times 10^5}{f(GHz)} K$$

Using a 7% bandwidth for the RF and a video bandwidth of 10^3 Hz, and

$$B = 7 \times 10^7 \, f(GHz) \text{ Hz}$$

$$B_v = 10^3 \text{ Hz}$$

$$k = 1.38 \times 10^{-23} \text{ joules/deg}$$

$$B_v/f_1 = 10^4$$

Substituting these values into the term corresponding to the detector noise, we obtain

$$A = \frac{1.35 \times 10^{-20} [1 + \frac{2000}{B_v} \ln(\frac{B_v}{f_1})] B}{[\gamma k B G (T_R + T_S + \Delta T_S)]^2} \approx \frac{80 \times 10^{10} f}{G^2 (4 \times 10^5 + \Delta T_S f + T_R f)^2} .$$

For the small signal case where $4 \times 10^5 >> (\Delta T_S + T_R) f$,

$$A = \frac{5f}{G^2}$$

Therefore, for a 3 dB degradation in the snr,

$$G^2 = 5f$$

and G = 5 dB at 2 GHz and 6.5 dB at 4 GHz.
For a gain of 31 dB as established previously[2], the degradation is

$$\frac{5f}{G^2} = 10^{-5} \text{ at 2 GHz and, equal to } 2 \times 10^{-5} \text{ at 4 GHz.}$$

For the 4-8 GHz octave,

$$T_S = 10^5 \left(\frac{4}{f}\right)^{-2.32} = 2 \times 10^4 \text{ K} \quad \text{at 8 GHz.}$$

For simplicity, we will evaluate the expression for the detector noise at 8 GHz since this is the worst case, i.e., the input signal is the smallest. Using the same parameters for the detector as above,

$$A \approx \frac{10^{11}}{G^2 (T_S+\Delta T_S+T_R)^2}$$

For $T_S = 2 \times 10^4 > \Delta T_S + T_R$ such that $(T_S+\Delta T_S+T_R)^2 \approx T_S^2$,

$$A \approx \frac{2.5 \times 10^2}{G^2}$$

For a 3 dB degradation in the snr, G = 16 or 12 dB. Using the gain of 28 dB established previously[2], the degradation is 6×10^{-4}.

Therefore we conclude that for these gains and input signals, the snr can be expressed as that of the DC radiometer

$$\frac{S^2}{N^2} = \frac{B\Delta T^2}{2B_V (T_S+\Delta T_S+T_R)^2}$$

In general, $T_S >> T_R$ and

$$\frac{S^2}{N^2} = \frac{B}{2B_V} \left(\frac{\Delta T_S}{T_S+\Delta T_S}\right)^2$$

The rms receiver fluctuation noise $\overline{\Delta T}$ is obtained by setting the snr equal to one, and solving for $\overline{\Delta T}$,

$$\overline{\Delta T} = (T_S+\Delta T_S)\sqrt{\frac{2B_v}{B}}$$

For a single section RC filter, $B_v = \frac{1}{4\tau}$ and

$$\overline{\Delta T} = \frac{T_S+\Delta T_S}{\sqrt{2B\tau}}$$

The fractional noise is

$$\frac{\overline{\Delta T}}{T_S+\Delta T_S} = \frac{1}{\sqrt{2B\tau}}$$

For $\tau = 2 \times 10^{-4}$ seconds and $B = 7 \times 10^{7}f$

$$\frac{\overline{\Delta T}}{T_S+\Delta T_S} \approx \frac{6\times10^{-3}}{\sqrt{f\,(GHz)}}$$

$\approx 4 \times 10^{-3}$ at 2 GHz

$\approx 3 \times 10^{-3}$ at 4 GHz

$\approx 2 \times 10^{-3}$ at 8 GHz

In all cases, the fluctuation noise is less than 1/2% of the input signal.

References

[1]"Hot Carrier Diode Video Detectors," Hewlett-Packard Application Note, 923.

[2]Appendix B, "Solar Receiver Dynamic Range Considerations,"

APPENDIX B

SOLAR RECEIVER

DYNAMIC RANGE CONSIDERATIONS

In Appendix C, the range of expected input temperatures and powers are calculated and tabulated for the quiet sun and for maximum recorded values of solar bursts. The dynamic range of the signals over the two octaves of interest, 2-4 GHz and 4-8 GHz, were 23 dB and 28 dB respectively. Based on these values of dynamic range and from the computed input powers, gains and dynamic range of the input amplifiers, i.e. wide band amplifiers, can be computed.

2-4 GHz. In this octave, the integrated input power for the active sun is -31 dBm. Transistor amplifiers in this octave have typical values of 1 dB gain compression for an output power of +10 dBm. Therefore if we use gain of 31 dB, the maximum output power is 0 dBm, leaving a 10 dB margin above the maximum recorded solar burst level. For the quiet sun, the output power is -23 dBm.

4-8 GHz. The dynamic range of the integrated input signal in this octave is 28 dB with a maximum input power of -28 dBm. Traveling wave tubes (TWT) having saturated output powers on the order of +13 dBm are available in this octave. This corresponds to 1 dB gain compression at an output level of +7 dBm. For a gain of 28 dB, the maximum output power is 0 dBm leaving 7 dB margin above the maximum recorded solar burst level. For the quiet sun, the output power is -28 dBm.

Detectors. The input power to the detectors will be considerably less than the wide band power because of the decreased bandwidth. In the 2-4 GHz region, the input power to the detectors is essentially constant since the bandwidth increases directly with frequency and the quiet sun temperature decreases with frequency directly. For large bursts, the solar temperature is essentially constant and the power to the detectors increases directly with frequency. This is true also for maximum values in the 4-8 GHz octave. At quiet sun levels in this octave, the power to the detectors decreases as $f^{-1.32}$.

Based on a 7% bandwidth and 10 channels per octave, channel widths and center frequencies were computed. Also, the input power and temperature to the detector systems were computed using the wide band amplifier gains established above. These data are tabulated below in Table 1.

Using the data in Table 1, the expected output voltages of the detectors were computed for the quiet sun. An insertion loss of 1.5 dB was assumed for the combination of the directional filter and the pin diode attenuator. Then, using the maximum expected output for the active sun, the open loop gain required to maintain a maximum error of 10% was calculated for the individual channels. A detector constant of 5000 mv/mw was used in the computations. The results are tabulated in Table 2. For smaller values of error in the output, the gain must be increased proportionally, e.g. to reduce the error to 5% all open loop gains must be doubled.

Table 1

Estimated Temperatures and Power per Channel

Channel	f(GHz)	Δf(MHz)	Quiet Sun				Active Sun	
			T_{in} (10^5K)	kTB (10^{-12}w)	P_{in} (dBm)	P_{out} (dBm)	P_{in} (dBm)	P_{out} (dBm)
1	2.07	145	1.93	386	-64	-33	-42	-11
2	2.22	155	1.80	385	-64	-33	-42	-11
3	2.38	167	1.68	387	-64	-33	-42	-11
4	2.55	179	1.57	388	-64	-33	-41.5	-10.5
5	2.73	191	1.47	387	-64	-33	-41	-10
6	2.92	204	1.37	386	-64	-33	-41	-10
7	3.13	219	1.28	387	-64	-33	-41	-10
8	3.36	235	1.19	386	-64	-33	-40.5	- 9.5
9	3.60	252	1.11	386	-64	-33	-40	- 9
10	3.86	270	1.03	384	-64	-33	-39.5	- 8.5
11	4.14	290	.934	374	-64	-36	-39.5	-11.5
12	4.44	310	.785	336	-65	-37	-39	-11
13	4.76	334	.668	308	-65	-37	-39	-11
14	5.10	358	.568	281	-65.5	-37.5	-38.5	-10.5
15	5.46	382	.485	256	-66	-38	-38	-10
16	5.84	408	.415	234	-66.5	-38.5	-38	-10
17	6.27	438	.351	212	-67	-39	-37.5	- 9.5
18	6.72	470	.299	194	-67	-39	-37.5	- 9.5
19	7.20	504	.254	177	-67.5	-39.5	-37	- 9
20	7.73	540	.219	163	-68	-40	-37	- 9

Table 2

Expected Detector Output Voltages and Required Loop Gains for a 10% Error (0.4 dB)

Channel	Detector V.[1] (milliv.)	Max. Req'd.[2] Attn. (dB)	Req'd. Output[3] (Volts)	Req'd. Gain ($\times 10^4$)
1	1.77	22	5.5	3.1
2	1.77	22	5.5	3.1
3	1.77	22	5.5	3.1
4	1.77	22.5	5.6	3.2
5	1.77	23	5.7	3.2
6	1.77	23	5.7	3.2
7	1.77	23	5.7	3.2
8	1.77	23.5	5.9	3.3
9	1.77	24	6.0	3.4
10	1.77	24.5	6.1	3.4
11	0.89	24.5	6.1	6.8
12	0.71	26	6.5	9.2
13	0.71	26	6.5	9.2
14	0.63	27	6.8	10.8
15	0.56	28	7.0	12.5
16	0.50	28.5	7.1	14.2
17	0.45	29.5	7.4	16.5
18	0.45	29.5	7.4	16.5
19	0.40	30.5	7.6	19.0
20	0.36	31	7.8	21.6

[1]Detector constant assumed to be 5000 mv/mw and an insertion loss of 1.5 dB assumed for the pin diode and directional filter.

[2]Based on the range of P_{out} for the sun as tabulated in Table 1.

[3]Attenuator constant of 4 dB/volt.

APPENDIX C

EXPECTED RECEIVER INPUT TEMPERATURES AND POWERS FOR A 2-8 GHz SOLAR RECEIVER USING THE 85-FOOT RADIO TELESCOPE

To determine the receiver requirements for the proposed solar receiver, the data discussed in the meeting of November 10, 1970 were put into the form of graphs, showing the range of (1) expected antenna temperatures, (2) power spectral density, and (3) dynamic range as a function of frequency. The integrated temperatures and input powers for the octaves 2-4 GHz and 4-8 GHz were also calculated. The data used for these calculations were given in the above meeting by FTH and are tabulated below.

Table 1

Maximum Recorded Solar Flux Densities and Equivalent Disc Temperatures.

Frequency	Mar 30, 1969		Feb 23, 1956		Quiet Sun
(GHz)	$Sx10^{18}$	T_{disc}	$Sx10^{18}$	T_{disc}	T_{disc}
9.4	2.5	$2.5x10^{7}$	3.5	$3.5x10^{7}$	$1.5x10^{4}$
3.75	3.0	$3.0x10^{7}$	2.0	$2.0x10^{7}$	$1 \cdot x10^{5}$
2.0	2.0	$2.0x10^{7}$	-	-	$2 \ x10^{5}$
1.0	0.65	$0.65x10^{7}$	-	-	$5 \ x10^{5}$

Figure 1 is a plot of the expected range of antenna temperature for the 85-foot antenna. This is based on the antenna temperature being equal to the disc temperature. Figure 2 is a similar plot but expessed in terms of the input power spectral density (dBm/MHz). Figure 3 is a plot of the dynamic range of the input signals as a function of frequency which ranges from about 10:1 at 1 GHz to about 2000:1 at 10 GHz. These graphs are all based on the average disc temperature, and as hot spots are resolved, the variation in temperature can be expected to be somewhat greater.

To simplify computations, approximations were obtained to express the disc temperature of the quiet sun for the two octaves of interest, 2-4 GHz and 4-8 GHz. These expressions are:

$$T_{disc} = \frac{4 \times 10^5}{f}, \qquad 1 < f < 4$$

$$T_{disc} = 10^5 \left(\frac{f}{4}\right)^{-2.32}, \qquad 4 < f < 8$$

where T_{disc} is in °K and f is in GHz.

Using these two expressions, the integrated temperature of the sun can be obtained for the octave of interest using the equation

$$\overline{T}_{disc} = \frac{1}{f_2 - f_1} \int_{f_1}^{f_2} T_{disc}(f)\, df$$

For 2-4 GHz,

$$\overline{T}_{disc}|_{2-4} = \frac{1}{2}\int_{2}^{4} \frac{4\times10^5}{f}\,df$$

$$= 2\times10^5[\ln 4 - \ln 2]$$

$$\overline{T}_{disc}|_{2-4} = 1.4\times10^5 \text{ K}$$

The integrated input power is

$$\overline{P}_{in}|_{2-4} = kTB = 1.38\times10^{-23} \times 1.4 \times 10^5 \times 2 \times 10^9$$

$$\overline{P}_{in}|_{2-4} = 3.9 \times 10^{-9} \text{ watts} = -54 \text{ dBm}$$

For the active sun, the maximum input power spectral density is approximately -64 dBm/MHz. Therefore

$$\overline{P}_{in\ max}|_{2-4} = -64 \text{ dBm/MHz} + 10 \log(4000-2000)$$

$$= -31 \text{ dBm}$$

Thus the dynamic range of the integrated input signal is 23 dB in the 2-4 GHz octave.

For 4-8 GHz,

$$\overline{T}_{disc}|_{4-8} = \frac{1}{4}\int_{4}^{8} 10^5 \left(\frac{f}{4}\right)^{-2.32} df$$

$$= 10^5\left[\frac{1}{-1.32}\left(2^{-1.32} - 1^{-1.32}\right)\right]$$

$$\overline{T}_{disc}|_{4-8} = 4.4\times10^4 \text{ K}$$

$$\overline{P}_{in}|_{4-8} = kTB = 1.38 \times 10^{-23} \times 4.5 \times 10^{4} \times 4 \times 10^{9}$$

$$\overline{P}_{in}|_{4-8} = 2.5 \times 10^{-9} \text{ watts} = -56 \text{ dBm}$$

For the active sun, using the maximum input power spectral density as -64 dBm/MHz,

$$\overline{P}_{in\ max}|_{4-8} = -64 \text{ dBm/MHz} + 10 \log(8000-4000)$$

$$\overline{P}_{in\ max}|_{4-8} = -28 \text{ dBm}$$

The dynamic range of the integrated input signal in the 4-8 GHz octave is 28 dB.

These integrated values for the input temperatures and powers are summarized in Table 2.

Table 2

Expected Integrated Antenna Temperatures and Input Powers

Octave		2-4 GHz	4-8 GHz
Quiet Sun	Temperature	1.4×10^{5} K	4.5×10^{4} K
	Input Power	-54 dBm	-56 dBm
Active Sun	Temperature	2.8×10^{7} K	2.8×10^{7} K
	Input Power	-31 dBm	-28 dBm
Dynamic Range		23 dB	28 dB

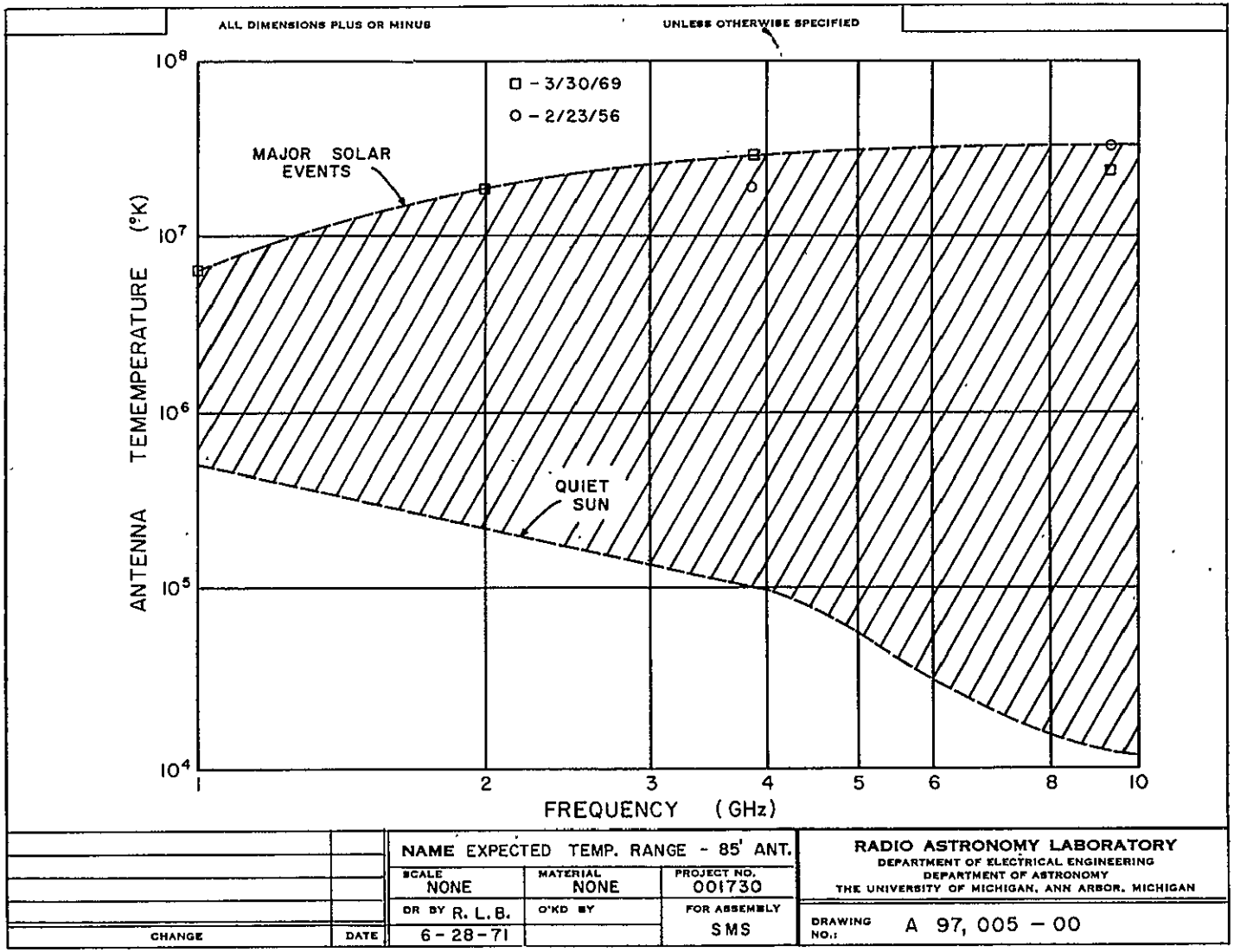

Figure 1. Expected Range of Antenna Temperatures for 85-foot Antenna

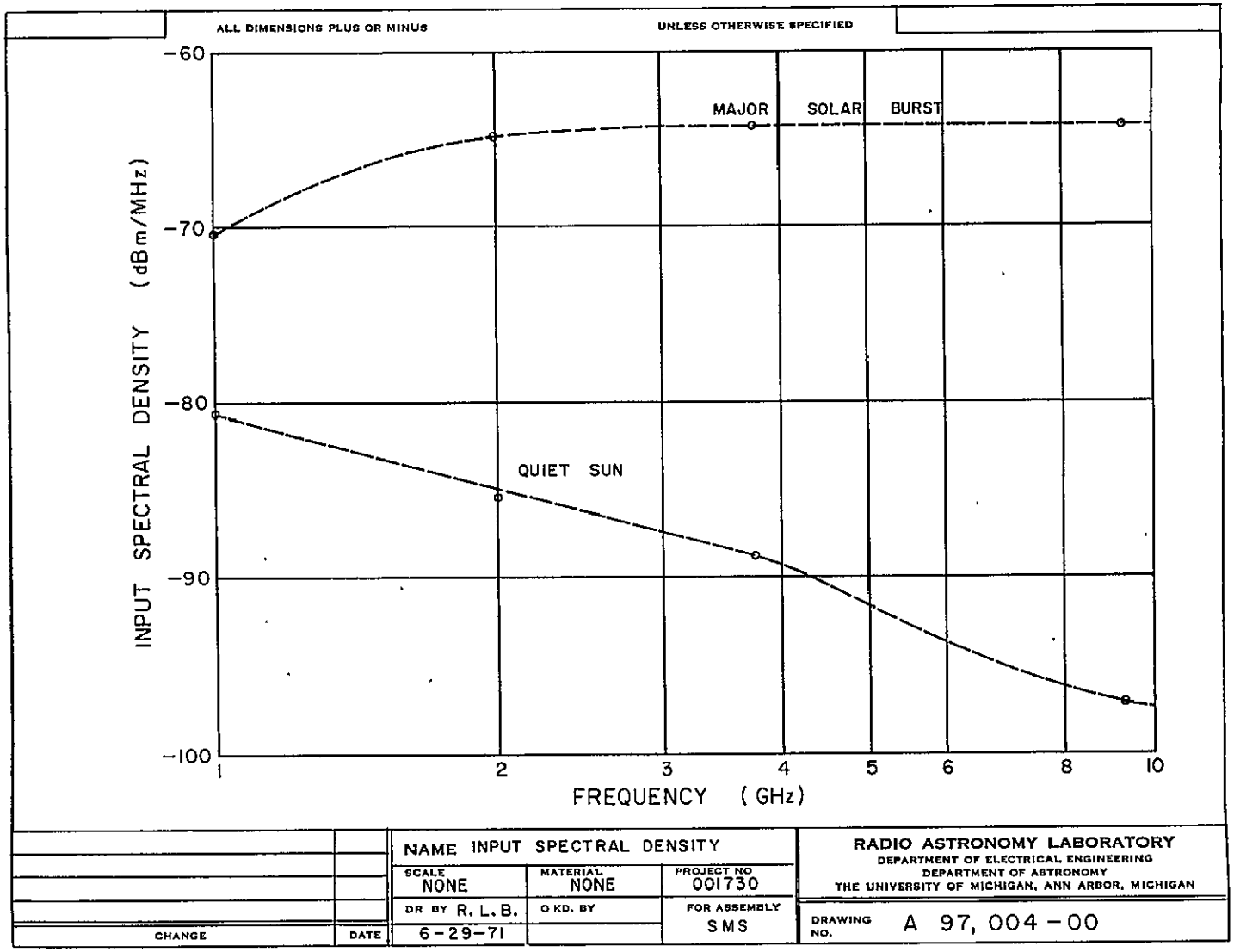

Figure 2. Input Power Spectral Density vs. Frequency

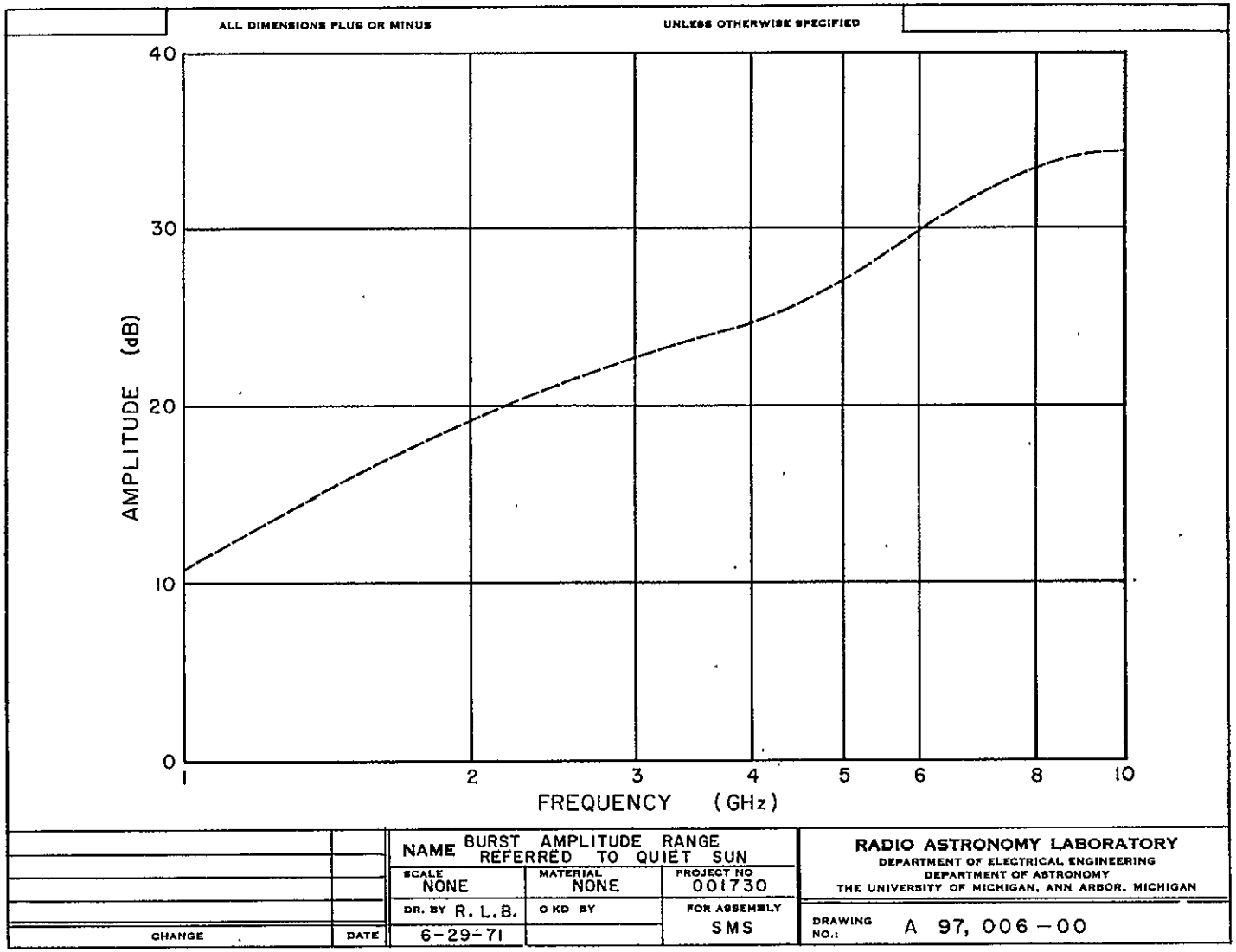

Figure 3. Range of Solar Burst Amplitude Referred to Quiet Sun (dB) vs. Frequency

APPENDIX D

EXPECTED RECEIVER INPUT TEMPERATURES AND POWERS FOR A 2-8 GHz SOLAR RECEIVER USING THE 28-FOOT RADIO TELESCOPE

This appendix details the expected range of input temperatures for the 2-8 GHz Solar Receiver in the same manner as outlined for the 85-foot radio telescope in Appendix C. Since the antenna beam of the 28-foot antenna is approximately 3 times wider than for the 85-foot antenna, the antenna beam will be larger than the solar disc at frequencies below 4.5 GHz. Therefore, the antenna temperature will vary as f^{-2} as compared to the 85-foot antenna at frequencies below 4.5 GHz. Using the same data as in Appendix C, the expected antenna temperatures were computed for the 28-foot antenna, and are tabulated below.

Table 1

Maximum Recorded Solar Flux Densities and Equivalent Antenna Temperatures

Frequency (GHz)	Mar 30, 1969		Feb 23, 1956		Quiet Sun
	$Sx10^{18}$	T_a(K)	$Sx10^{18}$	T_a(K)	T_a(K)
9.4	2.5	$2.8x10^6$	3.5	$3.9x10^6$	$1.5x10^4$
3.75	3.0	$3.3x10^6$	2.0	$2.2x10^6$	$7.5x10^4$
2.0	2.0	$2.2x10^6$	-	-	$4.0x10^4$
1.0	0.65	$0.72x10^6$	-	-	$2.0x10^4$

Figure 1 is a plot of the expected range of antenna temperatures for the 28-foot antenna. Figure 2 is a similar plot expressed as the input power spectral density (dBm/MHz), and Figure 3 is a plot of the expected dynamic range of the input signal as a function of frequency. The antenna temperature as a function of frequency for the quiet sun can be approximated by the following expressions.

$$T_a = 2 \times 10^4 \, f \qquad 1<f<4 \text{ GHz}$$

$$T_a = 7.6 \times 10^4 \left(\frac{f}{4.5}\right)^{-0.32} \qquad 4<f<4.5 \text{ GHz}$$

$$T_a = 7.6 \times 10^4 \left(\frac{f}{4.5}\right)^{-2.32} \qquad 4.5<f<8 \text{ GHz}$$

where T_a is in °K and f is in GHz.

Using these expressions the integrated antenna temperature for the quiet sun can be computed. For the 2-4 GHz octave,

$$\overline{T_a}\Big|_{2-4} = \frac{1}{2} \int_2^4 2 \times 10^4 \, f \, df$$

$$\overline{T_a}\Big|_{2-4} = 6 \times 10^4 \text{ °K}$$

The integrated input power is:

$$\overline{P_{in}}\Big|_{2-4} = kTB = 1.38\text{x}10^{-23} \times 6\text{x}10^4 \times 2\text{x}10^9$$

$$\overline{P_{in}}\Big|_{2-4} = 1.66 \times 10^{-9} \text{ w or } -58 \text{ dBm}$$

For the active sun, the integrated input temperature is approximately 2.8×10^6 °K, and the maximum input power is:

$$\overline{P_{in}}\Big|_{\text{max } 2-4} = kTB = 1.38\text{x}10^{-23} \times 2.8\text{x}10^6 \times 2\text{x}10^9$$

$$\overline{P_{in}}\Big|_{\text{max } 2-4} = 7.75 \times 10^{-8} \text{ w or } -41 \text{ dBm.}$$

Thus the dynamic range of the integrated input signal is 17 dB for the 2-4 GHz octave.

For the 4-8 GHz octave, the integrated antenna temperature for the quiet sun is:

$$\overline{T_a}\Big|_{4-8} = \frac{7.6\times10^4}{4}\left[\int_4^{4.5}\left(\frac{f}{4.5}\right)^{-.32}df + \int_{4.5}^{8}\left(\frac{f}{4.5}\right)^{-2.32}df\right]$$

$$\overline{T_a}\Big|_{4-8} = 4.35 \times 10^4 \ ^\circ K$$

$$\overline{P_{in}}\Big|_{4-8} = kTB = 1.38\times10^{-23} \times 4.35\times10^4 \times 4\times10^9$$

$$\overline{P_{in}}\Big|_{4-8} = 2.4 \times 10^{-9} \text{ w or } -56 \text{ dBm}$$

For the active sun, the integrated input temperature is approximately 3.3×10^6 °K, and the maximum input power is:

$$\overline{P_{in\ max}}\Big|_{4-8} = 1.39\times10^{-23} \times 3.3\times10^6 \times 4\times10^9$$

$$\overline{P_{in\ max}}\Big|_{4-8} = 1.82 \times 10^{-7} \text{ w or } -37 \text{ dBm}$$

The dynamic range of the integrated input signal for the 4-8 GHz octave is 19 dB.

These integrated values for the input temperatures and powers are summarized in Table 2.

Table 2

Expected Integrated Antenna Temperatures and Input Powers

Octave		2-4 GHZ	4-8 GHz
Quiet Sun	Temperature	6×10^4 K	4.35×10^4 K
	Input Power	-58 dBm	-56 dBm
Active Sun	Temperature	2.8×10^6K	3.3×10^6 K
	Input Power	-41 dBm	-37 dBm
Dynamic Range		17 dB	19 dB

Dynamic Range Considerations (Re: Appendix B)

2-4 GHz. The input power for the active sun is -41 dBm, and if the gain of the wide band amplifier is set at 40 dB, the maximum output power is -1 dBm. This leaves a margin of 11 dB below the 1 dB gain compression point. For the quiet sun, the output power is -18 dBm. In this octave, the power in the filter channels vary as f^2 since both the input power and bandwidth vary as f^1. The power to the detectors varies approximately from -31 dBm to -25 dBm for the quiet sun, from 2-4 GHz. For the active sun, the power varies from -14 dBm to -9 dBm. Since the minimum value of power is greater than that for the 85-foot antenna, the loop gains of the pin attenuator circuits are more than adequate for use on the 28-foot antenna.

4-8 GHz. If the gain of the wide band preamplifier for this octave is set at 34 dB, the output power is -3 dBm. This output power is 10 dB below the 1 dB gain compression point for the planned TWT. The output power for the quiet sun is -22 dBm.

The power to the detectors varies from about -31 dBm at 4 GHz to -34 dBm at 8 GHz for the quiet sun. For major solar bursts, the expected power varies from -15 dBm to -10 dBm. Again, the loop gains of the pin diode attenuator circuits are more than adequate for use on the 85-foot antenna.

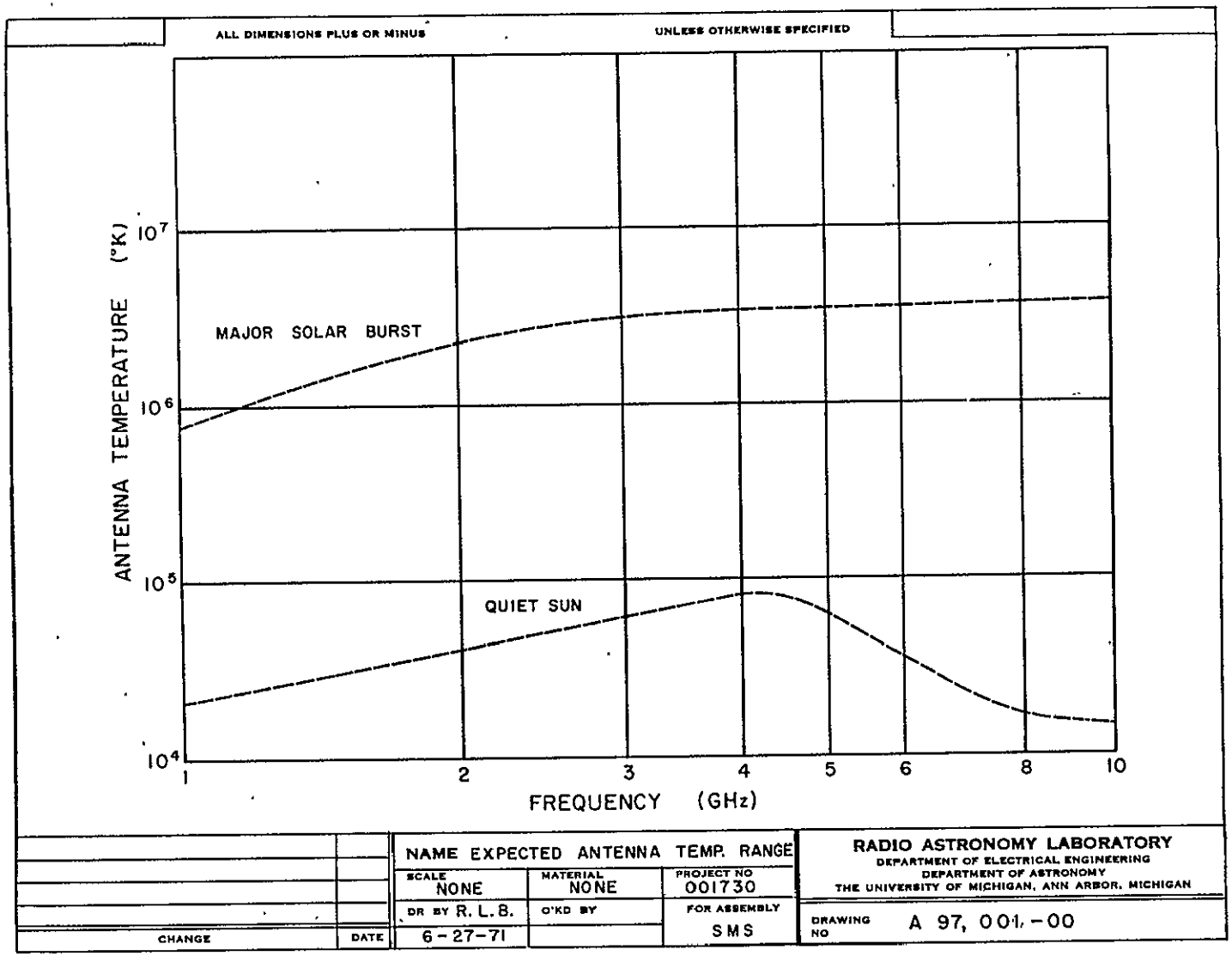

Figure 1. Expected Range of Antenna Temperatures for the 28-foot Antenna

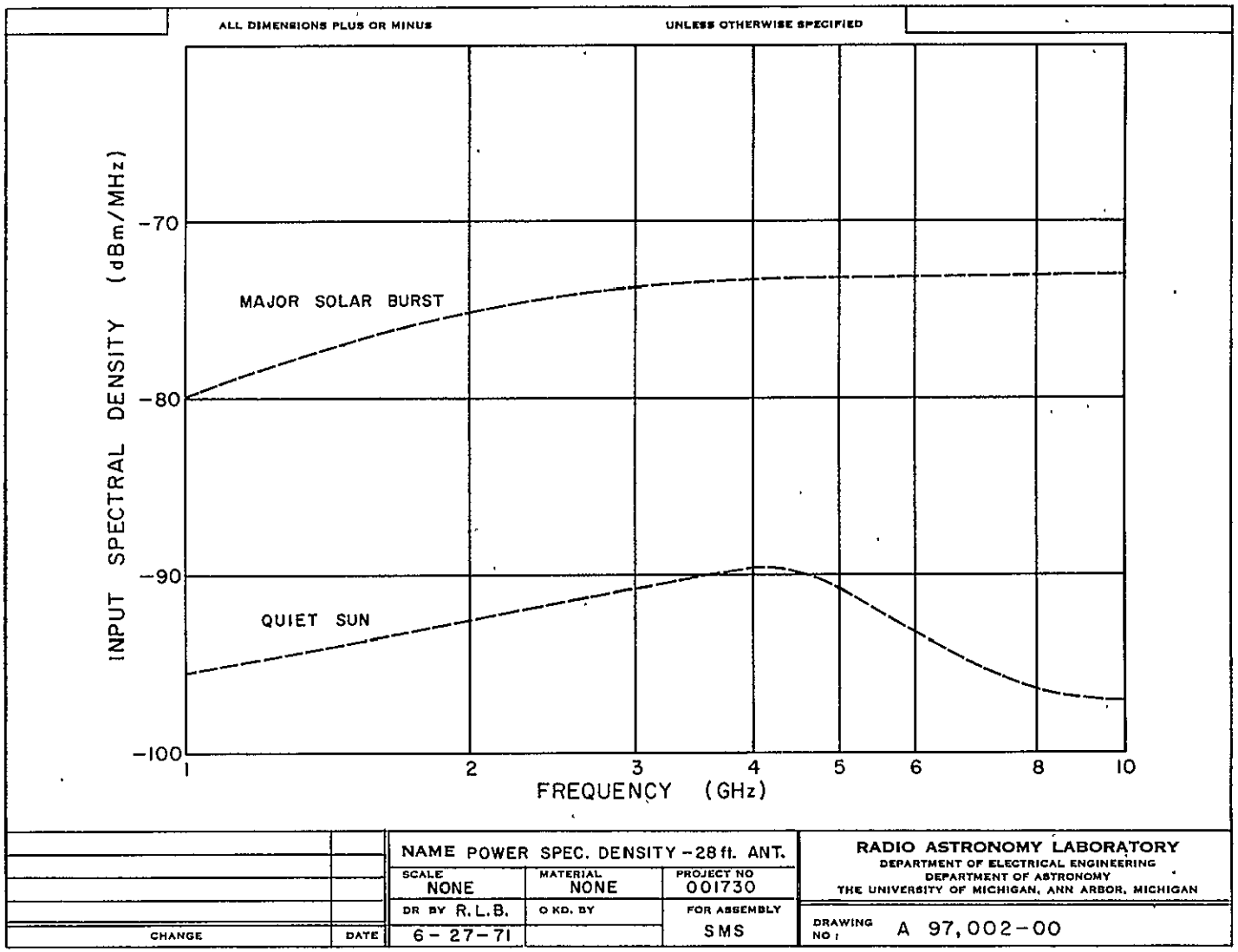

Figure 2. Input Power Spectral Density vs. Frequency for the 28-foot Antenna

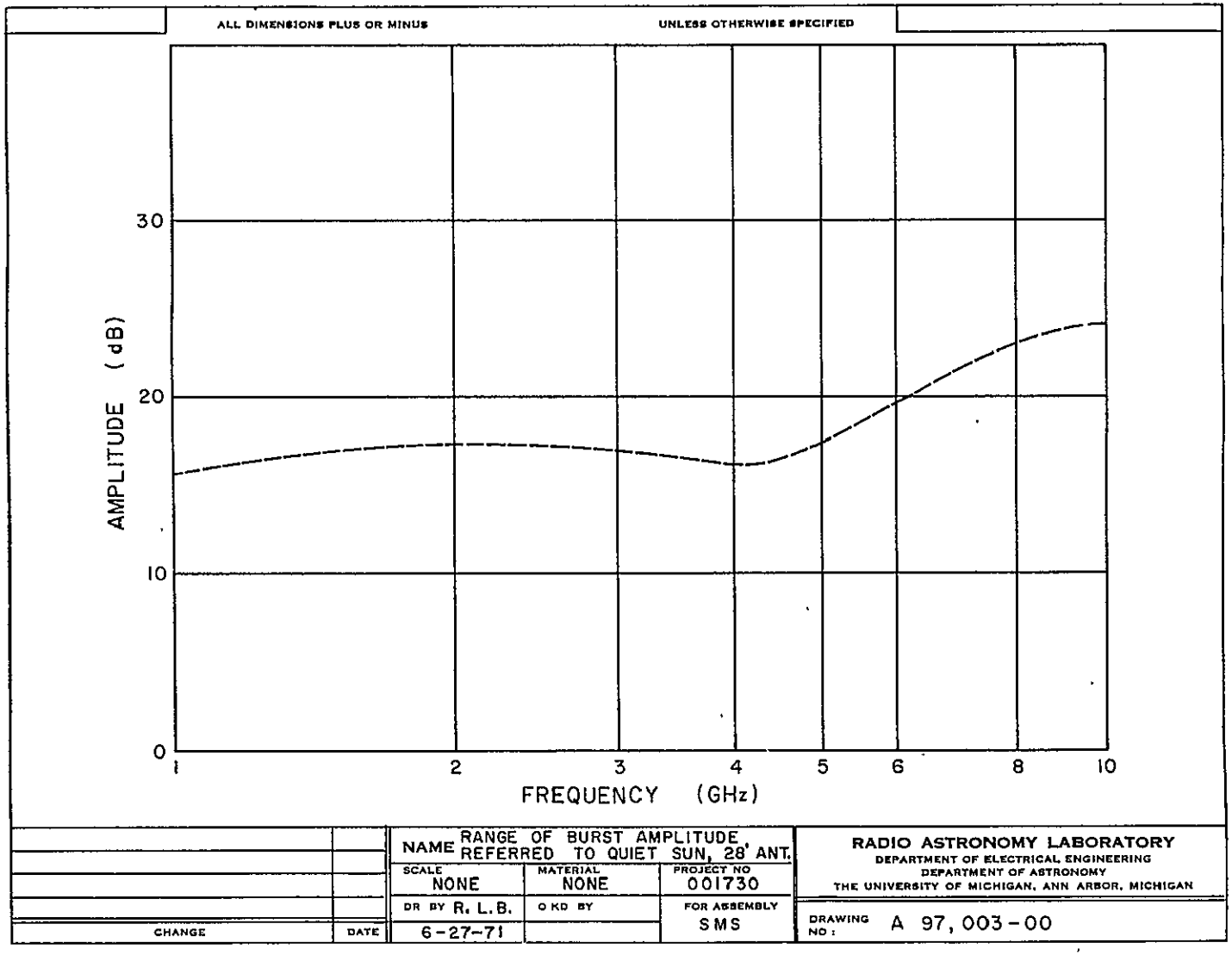

Figure 3. Range of Solar Burst Amplitude Referred to the Quiet Sun vs. Frequency for the 28-foot Antenna

APPENDIX E

Resolution, Dynamic Range, and Number of Bits, for a Logarithmic Instrument with Digitized Output

Consider an instrument whose transfer characteristic is

$$V = a \log T + b \tag{1}$$

where T is an input stimulus, and V is an output voltage to be digitized. T and V have ranges:

$$T_{min} \leq T \leq T_{max}, \quad 0 \leq V \leq V_{max}.$$

V is to be quantized by converting it to a binary number of n bits. We wish to find ΔT the resolution element in T corresponding to the resolution element ΔV.

Convert (1) to natural logs:

$$V = \frac{a}{2.302} \ln T + b$$

Differentiate:

$$dV = \frac{a}{2.302} \frac{dT}{T}$$

Let V be digitized with a precision of n bits. Then the quantum in V is

$$\Delta V = \frac{V_{max}}{2^n} = \frac{a}{2.302} \frac{\Delta T}{T}$$

$$\frac{\Delta T}{T} = \frac{2.302}{a} \frac{V_{max}}{2^n} \tag{2}$$

We can find a by substituting the boundary condition in (1):

$$V_{max} = a \log T_{max} + b$$

$$0 = a \log T_{min} + b$$

$$V_{max} = a \log \frac{T_{max}}{T_{min}}$$

$$a = \frac{V_{max}}{\log \frac{T_{max}}{T_{min}}} \tag{3}$$

Also, solve for B:

$$b = -a \log T_{min} = - \frac{V_{max}}{\log \frac{T_{max}}{T_{min}}} \log T_{min}$$

Substitute (3) in (2):

$$\frac{\Delta T}{T} = \frac{2.302}{2^n} \log \frac{T_{max}}{T_{min}}$$

If DR (db) is the dynamic range, expressed in db, then

$$\log \frac{T_{max}}{T_{min}} = \frac{1}{10} \text{ DR (db)}, \quad \text{and}$$

$$\frac{\Delta T}{T} = \frac{0.2302}{2^n} \text{ DR (db)}$$

If $\Delta T/T$ is expressed in percentage,

$$\frac{\Delta T}{T} (\%) = \frac{23.02}{2^n} \text{ DR (db)}.$$

TABLE I

Resolution in Temperature [$\Delta T/T(\%)$] as a Function of Dynamic Range [DR(db)] and Number of Bits (n)

DR(db)	n = 10	n = 11	n = 12
20	0.45	0.22	0.11
30	0.67	0.34	0.17
40	0.90	0.45	0.22
50	1.12	0.56	0.28
60	1.35	0.67	0.34
70	1.57	0.79	0.40
80	1.80	0.90	0.45

The parameters a and b may be evaluated in terms of DR(db):

$$a = \frac{10\ V_{max}}{DR(db)}$$

$$b = -a \log T \text{ min}$$

TABLE II

Parameters a and b vs. DR(db), for V_{max} = 10 volts, $T_{min} = 10^4 °K$

DR(db)	a	b
20	5.00	-20.00
30	3.33	-13.33
40	2.50	-10.00
50	2.00	-8.00
60	1.67	-6.67
70	1.43	-5.72

ALL DIMENSIONS PLUS OR MINUS UNLESS OTHERWISE SPECIFIED

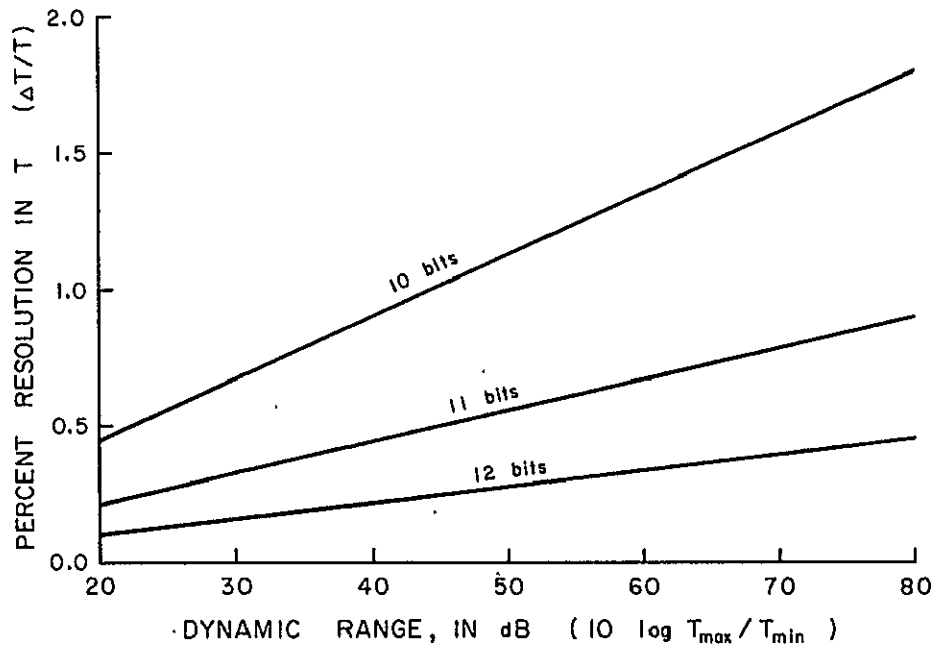

		NAME RESOLUTION IN T			RADIO ASTRONOMY LABORATORY DEPARTMENT OF ELECTRICAL ENGINEERING DEPARTMENT OF ASTRONOMY THE UNIVERSITY OF MICHIGAN, ANN ARBOR, MICHIGAN
		SCALE NONE	MATERIAL NONE	PROJECT NO. 001730	
		DR BY R.L.B.	CK'D. BY	FOR ASSEMBLY SMS	DRAWING NO. A 97, 008-00
CHANGE	DATE	6-29-71			

Resolution in T, as a Function of Dynamic Range and Number of Bits

APPENDIX F

Estimated Receiver Cost

Item	No. Req'd.	Description	Price Unit	Price Total	Delivery Days
1	1	Antenna Feed (See Section 4.1.1)			-
2	1	Quadrature Hybrid		$250	30
3	2	Diplexer	$ 880	1760	60-75
4	4	Directional Couplers	125	500	30
5	2	Ferrite Switch	1400	2800	45-60
6	2	Transistor Amplifier		3200	30
7	1	Traveling Wave Tube		4100	30
8	1	Attenuator		250	30
9	20	Pin Diode Attenuators	350	7000	45-60
10	20	Detector Diodes	10	200	30
11	80	IC Operational Amplifiers		700	30
12	8	Coaxial Switches	264	1056	30
13	20	Filters	50	1000	
14	1	2-4 GHz TDA		4410	60-90
15	1	4-8 GHz		5100	60-90
16		Power Supplies		700	
17		Packaging, cabling, connectors, and miscellaneous supplies		2000	
18	4	Diode Noise Sources	50	200	
19	1	High Level Noise Generator		5200	
		TOTAL COST		$40,426	

Description of Major Receiver Components

Item 1. Antenna Feed (See Section 4.1.1)

Type:
Gain: 7 dB nominal
Frequency Range: 2-8 GHz
Manufacturer:
Model:
Price:
Delivery: 60-90 days

Item 2. Quadrature Hybrid

Type: 3 dB 90° Hybrid
Frequency Range: 2-11 GHz
Manufacturer: Anaren Microwave Inc.
Model: 10310-3
Price: $250
Delivery: Stock to 30 days

Item 3. Diplexer

Frequency Range:
Input: 2-8 GHz
Output 1: 2-4 GHz
Output 2: 4-8 GHz
Insertion Loss: 1 dB max.
Manufacturer: Microphase Corp.
Price: $880
Delivery: 60-75 days

Item 4. Directional Couplers

Frequency Range: 2-4 GHz and 4-8 GHz
Manufacturer: Anaren Microwave, Inc.
Model: 10016 Series (2-4 GHz)
10017 Series (4-8 GHz)
Price: 10016 Series $120
10017 Series $130
Delivery: Stock to 30 days

Item 5. Ferrite Switches

Frequency Range: 2-4 GHz and 4-8 GHz
Type: Coaxial Pulse Latched
Insertion Loss: 0.6 dB max.
Isolation: 18 dB min.
Manufacturer: Western Microwave Laboratories, Inc.
Model: 6L-2040 (2-4 GHz)
6L-4080 (4-8 GHz)
Price: $1400
Delivery: 45-60 days

Item 6. Transistor Amplifier

Frequency Range: 2-4 GHz
Gain: 40 dB min.
Noise Figure: 7.5 dB max.
Output Power at 1 dB Gain Compression: +10 dBm
Manufacturer: Avantek
Model: AM-4051M followed with an AMT-4002M
Price: $3200
Delivery: 30 days

Item 7. Traveling Wave Tube

Frequency Range: 4-8 GHz
Gain: 40 dB min.
Noise Figure: 8.5 dB max.
Saturated Output Power: +13 dBm min.
Manufacturer: Microwave Electronics Corp.
Model: M9152A
Delivery: 30-45 days
Price: $4100

Item 8. Attenuator

Frequency Range: 2-4 GHz
Attenuation: 0-20 dB
Insertion Loss: 0.5 dB max.
Flatness: ±1.5 dB max.
Manufacturer: ARRA, Inc.
Model: 4674-20F
Price: $250
Delivery: Stock to 30 days

Item 9. Pin Diode Attenuators

Frequency Range: 2-8 GHz
Bandwidth: 10% of center Frequency
Attenuation: 40 dB min.
Insertion Loss: 1.0 dB max.
Max Voltage Req'd: 10 volts
Manufacturer: Alpha Microwave or General Microwave
Model: Alpha ----
General M186A
Price: Alpha $350 (Linearized)
General $250
Delivery: 45-60 days

Item 10. Detector Diodes

Manufacturer: Hewlett Packard
Type: 5082-2759
Price: $9.35 (10-99)
Delivery: Stock to 30 days

Item 11. Operational Amplifiers

Type: Low Noise Integrated Circuit
Manufacturer: RCA, Fairchild, etc.
Price: Average about $7-9
Delivery: Stock to 30 days

Item 12: Coaxial Transfer Switch

Frequency Range: DC-12
Insertion Loss: 0.3 dB (2-4 GHz) max.
0.4 dB (4-8 GHz) max.
Isolation: 60 dB min.
Manufacturer: Teledyne Microwave (Quantatron)
Price: $264
Delivery: Stock to 30 days

Item 13: Directional Filters

Frequency Range: 2-8 GHz

Bandwidth: 7% of Center Frequency

Insertion Loss: 1 dB max.

Manufacturer: UM/RAO

Price: $50 Material Costs

Item 14. 2-4 GHz Tunnel Diode Amplifier

Frequency Range: 2-4 GHz

Gain: 14 dB min.

Gain Variation with Frequency: Less than 3 dB

Noise Figure: 6.0 dB max.

Proportional Heater Control

Power: 115 VAC

Manufacturer: Aertech

Price $4410

Delivery: 60-90 days

Item 15. 4-8 GHz Tunnel Diode Amplifier

Frequency Range: 4-8 GHz

Gain: 15 dB min.

Gain Variation with Frequency: Less than 3 dB

Noise Figure: 6.0 Max.

Proportional Heater Control

Power: 115 VAC

Manufacturer: Aertech

Price $5100

Delivery: 60-90 days

Item 16. Power Supplies

Several Power Supplies will be required for the receiver. Estimated cost of power supplies $700 total. (Approximately 7 supplies at $100 each.)

Item 17. Packaging, cabling, connectors, hardware, and miscellaneous supplies.

Estimated Cost: $2000

Item 18. Diode Noise Source

Frequency Range: 2-4 GHz and 4-8 GHz

Excess Noise: Approximately 25 dB above 290 K (10^5K)

Manufacturer: UM/RAO

Price: $50 Material Costs

Item 19. High Level Noise Generator

MJ2207E TWT	$1400
Power Supply	350
Transistor Amplifier	2200
Pin Diode Attenuator	250
Power Supply	50
Detectors	300
Directional Couplers	300
Computer Interface	200
AGC Amplifiers and Power Supplies	100
Miscellaneous Parts and Hardware	50
Total	$5200

APPENDIX G

ESTIMATED COST OF THE DATA ACQUISITION EQUIPMENT

The estimated cost of the data acquisition subsystem is based upon the PDP8-E, by Digital Equipment Corporation, as listed below. This equipment was chosen for a representative cost estimation only and is not necessarily the equipment which will be purchased. The primary function of this equipment is to control the timing, sequencing, and operation of the instrument as well as the formatting of the recorded data. Special purpose equipment could be custom designed and built to perform these functions, but the cost would be greater and the equipment less versatile than the PDP8-E type subsystem.

Data Acquisition Equipment Components

1 PDP8/EA, including: 1 KK8-E Central Processor 1 MM8-E 4K Core Memory 1 KC8-EA Programmer's Console 1 KL8-E Console TTY Control 1 Power Supply, Chassis and Omnibus with 20 Slots, H960 cabinet	$ 5,640
1 KE8-E Extended Arithmetic Element	1,000
1 M8-E 4K Memory Extension	3,000
1 KP8-E Power Fail Detector and Auto Restart	250
1 LT35DC Heavy-Duty Teletype	4,500
1 AD01-AP Multiplexer and A/D Converter	2,400
1 AH04 Sample-Hold for A/D Converter	300
8 A124 4-Channel Multiplexer Module, $60 each	480
1 VT01 Storage Screen Display	3,000
1 VS8-E Control for Storage Screen Display	2,000
1 KA8-E External Interface for Positive I/0	500
2 KD8-E Data Break Interface, $500 each	1,000
1 DR8-EA 12-Channel Digital Interface	250
4 TU10-E Magnetic Tape Transport, $6950 each	27,800
2 TC58 Controller for TU10-E, $6800 each	13,600
TOTAL	$65,720

References

Acton, L.W. (1968) "X-Ray and Microwave Emission of the Sun with Special Reference to the Events of July, 1961," The Astrophysical Journal 152, 305-317.

Arnoldy, R.L., Kane, S.R. and Winckler, J.R. (1967) "A Study of Energetic Solar Flare X-Rays," Solar Physics, 2, 171-178.

Badillo, V.L., Castelli, J.P. (1969) "The Proton Flare of 9 June 1968," Astrophysical Letters 4, 59.

Bratenahl, A. and Yeates, C.M. (1970) "Experimental Study of Magnetic Flux Transfer at the Hyperbolic Neutral Point," Physics of Fluids 13, 2696-2709.

Cribbens, A.H. and Matthews, P.A. (1969) "Periodic Structure in Solar Radio Bursts and Its Relation to Burst Energy," Nature 22, 158-159.

Friedman, M. and Hamberger, S. M. (1968) "On the Neutral-Point Region in Petschek's Model of Magnetic-Field Annihilation," The Astrophysical Journal 152,667-669.

Harries, J.R. (1970) "Solar X-Ray Bursts and Their Relation to H_α and Microwave Emissions," Solar Physics 13, 467-470.

Holt, S. and Ramaty, R. (1969) "Microwave and Hard X-Ray Bursts from Solar Flares," Solar Physics 8, 119-141.

Janssens, T.J. and White III, K.P. (1969) "Microwave Pulse Trains Observed Before and During a Solar Flare," The Astrophysical Journal 158, L127-L128.

Kahler, S.W., Meekins, J.F., Kreplin, R.W. (1970) "Temperature and Emission-Measure Profiles of Two Solar X-Ray Flares," The Astrophysical Journal 162, 293-304.

Kane, S.R. and Donnelly, R.F. (1971) "Impulsive Hard X-Ray and Ultraviolet Emission During Solar Flares," The Astrophysical Journal 164, 151-163.

Kaufmann, P. (1969) "Unpolarized Impulsive Solar Bursts Observed at 7 GHz," Solar Physics 9, 166-172.

Kaufmann, P., Matsuura, O.T., Marques dos Santos, P. (1970) "Polarization Changes with Time During Solar Microwave Impulsive Bursts," Solar Physics 14, 190-195.

Kaufmann, P., Matsuura, O.T., Monte Mascaro, A.C., Mendes, A.M., (1968) "Polarization Bursts in the Sun Observed at Microwave Frequencies," Nature 220, 1298-1300.

Kundu, Mukul R. (1964) "Solar Radio Astronomy," Report No. 64-4, University of Michigan Radio Astronomy Observatory;

(1965) "Solar Radio Astronomy," Interscience Publishers, New York. See in particular Chapter 13.

Lieholm, H.B., (1965) "Radiation from Electrons in a Magnetoplasma," Radio Science 69D, 741-766.

O'Dell, S.L., and Sartori, L. (1970), "Low Frequency Cutoffs in Synchrotron Spectra," The Astrophysical Journal 162, L37-L42.

Parks, G.K. and Winckler, J.R. (1969) "Sixteen-Second Periodic Pulsations Observed in the Correlated Microwave and Energetic X-Ray Emission from a Solar Flare," The Astrophysical Journal 155, L117-L120.

Peterson, L.E. and Winckler, J.R. (1959) "Gamma Ray Burst From a Solar Flare," Journal of Geophysical Research 64, 697-707.

Petschek, H.E. (1964) "Magnetic Field Annihilation," in AAS-NASA Symposium on the Physics of Solar Flares," U.S. Government Printing Office, Washington D.C., NASA SP-50.

Ramaty, R. and Lingenfelter, R.E. (1967) "The Influence of the Ionized Medium on Synchrotron Emission Spectra in the Solar Corona," Journal of Geophysical Research 72, 879-883.

Sakurai, K. and Ogawa, T. (1969) "Radiation Fields of Energetic Electrons in Helical Orbits within a Magnetoactive Plasma," Planet Space Sci. 17, 1449-1458.

Strauss, F.M. and Papagiannis, M.D. (1971) "A Model for the Source of Solar-Flare X-Rays," The Astrophysical Journal 164, 369-378.

Takakura, T. and Kai, K. (1966) "Energy Distribution of Electrons Producing Microwave Impulsive Bursts and X-Ray Bursts from the Sun," Publications of the Astronomical Society of Japan 18, 57-76.

Takakura, T. and Scalise, E. Jr. (1970) "Gyro-Synchrotron Emission in a Magnetic Dipole Field for the Application to the Center-to-Limb Variation of Microwave Impulsive Bursts," Solar Physics 11, 434-455.

Tanaka, H. and Enomé, S. (1970) "High Resolution Observations of Solar Microwave Bursts," Nature 225, 435-437.